Development and analysis of ECG data compression schemes

Hao, Yanyan

2007

Hao, Y. (2007). Development and analysis of ECG data compression schemes. Master's thesis, Nanyang Technological University, Singapore.

https://hdl.handle.net/10356/4342

https://doi.org/10.32657/10356/4342

Development and Analysis of ECG Data Compression Schemes

Hao Yanyan

School of Electrical & Electronic Engineering

A thesis submitted to the Nanyang Technological University
in fulfilment of the requirement for the degree of
Master of Engineering

2007

Acknowledgements

I wish to express my gratitude to all of the following people who helped to make this thesis possible:

The first and most important is my supervisor Assistant Professor Pina Marziliano, for giving me a lot of knowledge, ideas, assistance and support.

My BMERC colleague, Lu Rui, for helping me in research and daily life.

My NTU friends, Liu Bing, Shi Xiaomeng, Cao Qi, Liu Fangrui, Shi Minlong, Liu Wen, who were like a second family to me.

My parents and brother, for their patience and support.

Summary

Important clinical information of the human heart can be observed from electrocardiogram (ECG) signals. Since ECG signals are usually recorded in a long period of time for clinical diagnosis, huge amount of data is produced everyday for storage and transmission, thus to accurately and efficiently compress ECG data is of vital importance.

The algorithms developed so far fall into three groups: direct data compression methods, transformation methods and parametric methods. These methods have become essential in a large variety of applications, from remote clinical diagnosis to ambulatory recording. The purpose of our research is to develop encoding and decoding schemes for ECG data compression and reconstruction.

Firstly, although much work has been devoted to the development of ECG data compression algorithms, the existing ones do not fully take advantage of the interbeat correlation of the ECG signal. In our study, the correlation between successive beats is utilized to detect and eliminate redundancies in the original signal. Moreover, pattern matching and residual coding are used in order to achieve a high compression ratio. Recommendation for future work is to improve the present algorithm by replacing the one-stage pattern matching unit with a two-stage one. Besides single-channel signals, multi-channel ECG data and more efficient compression schemes can also be investigated in the future.

Secondly, by modelling the ECG signal as the sum of a bandlimited signal and

nonuniform linear spline, we have sampled and decompressed the ECG as a signal with finite rate of innovation. The peak area of ECG signal is approximated as a nonuniform linear spline, and the remaining part of the signal is approximated as a bandlimited signal. The ECG signal is then sampled at the rate of innovation and the results show that the morphological information of the ECG signal is well preserved in the reconstruction. Optimal modelling of an ECG as a signal with finite rate of innovation can be investigated in the future to yield more efficient compression and accurate reconstruction.

Table of Contents

List of Figures

List of Tables

Chapter 1

Introduction

1.1 Motivation

The electrocardiogram (ECG) is the electrical manifestation of the contractile activity of the heart and can be recorded fairly easily by placing noninvasive electrodes on the limbs and chest. Each heartbeat produces a sequence of electrical waves. Since the ECG signal records the electrical potential at the electrode (or the potential difference between two electrodes) induced by the presence of time-varying electrical activity in cardiac muscle, by examining the shape of the ECG waveforms, a physician can obtain considerable insight about whether the contractions of the heart are occurring normally or abnormally. The signal can be measured as a multi-channel signal, or as a single-channel signal, depending on the application. In the application of standard clinical ECG, 12 different ECG leads (channels) are recorded from the body surface of a resting patient. In the application of arrhythmia analysis, one or two ECG leads are recorded to look for life-threatening disturbances in the rhythm of the heartbeat.

Since many aspects of the physical condition of the human heart are reflected in the waveforms of ECG, it is important to record the patient's ECG for a long period of time for clinical diagnosis. Normally, a 24 hour or even longer duration recording is desirable for doctors to detect the human body's abnormalities or disorders, which can always be required in clinical applications such as telemedicine. This produces a large volume of ECG data everyday for storage and transmission. Storage requirement or transmission bandwidth for ECG signal can range from 26 MB/day (with one lead and a resolution of 12 bits sampled at 200 Hz) to 138 MB/day (with two leads and a resolution of 16 bits sampled at 400 Hz). The continuing proliferation of computerized ECG processing systems along with the increased feature performance requirements and demand for lower cost medical care have mandated reliable, accurate and more efficient ECG data compression techniques.

The need for ECG data compression exists in many transmitting and storage applications. The practical importance and effect of ECG data compression has become evident in many aspects of computerized electrocardiography including:

1. Increased storage capacity of ECG signal as databases for subsequent comparison or evaluation;

2. Feasibility of real-time ECG transmission for remote clinical diagnosis;

3. Improved functionality of ambulatory ECG monitors and recorders.

1.2 Objectives

Conceptually, data compression is the process of detecting and eliminating redundancies in a given data set. The main goal of any compression technique is to achieve maximum data volume reduction while preserving the significant signal morphology features upon reconstruction. Compression techniques can be divided into two categories: lossless compression and lossy compression. In most ECG applications, the lossless methods do not provide sufficient compression, and distortions are to be expected in practical ECG compression systems.

Data compression algorithms must also represent the data with acceptable fidelity. In ECG and other biomedical data compression, the clinical acceptability of the reconstructed signal has to be determined through visual inspection from medical experts. However, clinically acceptable quality is neither guaranteed by a low nonzero residual nor ruled out by a high numerical residual.

The aim of our study is to develop systems which allow distortion for ECG compression and reconstruction with the following features:

1. Detection and elimination of redundancies in the ECG data;
2. Efficient compression of the ECG data after removing the redundancies;
3. Reconstruction of the original signal with a low distortion;
4. Diagnostic information is well preserved in the reconstructed signal.

1.3 Major Contributions of the Thesis

The fundamentals of data compression and conventional methods of ECG compression have been reviewed in the first part of the thesis. The conventional methods have been classified into three categories, which are discussed in detail. Then two methods have been proposed for ECG compression, both of which have yielded good compression ratio with low distortion.

Firstly, a novel coding scheme for ECG data compression is proposed in this thesis. Following beat delineation, the periods of the beats are normalized by multirate processing. Amplitude normalization is performed afterwards, and the discrete wavelet transform is applied to each normalized beat. Due to the period and amplitude normalization, the wavelet transform coefficients bear a high correlation across beats. To increase the compression ratio, a pattern matching unit is utilized, and the residual sequence obtained is further encoded. The difference between the actual period and the standard period, and the amplitude scale factor are also retained for each beat. At the decoder, the inverse wavelet transform is computed from the reconstructed wavelet transform coefficients. The original amplitude and period of each beat are then recovered. The simulation results show that our compression algorithm achieves a significant improvement in the performance of compression ratio and error measurement.

Secondly, by modelling the ECG signal as the sum of bandlimited and nonuniform linear spline which contains a finite rate of innovation (FRI), sampling theory is applied to achieve effective compression and reconstruction of the ECG signal.

The simulation results show that the performance of the compression of ECG as a signal with FRI is quite satisfactory in preserving the diagnostic information as compared to the classical sampling scheme which uses the sinc interpolation in the reconstruction.

1.4 Organization of the Thesis

The rest of this thesis is organized as follows: A review of the conventional ECG data compression techniques is given in Chapter 2; a detailed discussion of a novel wavelet-based pattern matching method for ECG data compression is given in Chapter 3; compression of ECG as signals with finite rate of innovation is presented in Chapter 4; finally, conclusions along with recommendations for future research are given in Chapter 5.

Chapter 2

Conventional Methods for ECG Data Compression

2.1 Data Compression

Digital coding is the process, or sequence of processes, that leads to digital representations (sequences of binary digits) of the source signal (mostly analog sources). The benefits of digital representation are well known: low sensitivity to transmission noise, effective storage, ability to multiplex, error-protection and more.

One of the main goals in digital coding of waveforms is reduction of the bit rate, which is required to transmit a certain amount of information. The process of bit rate reduction is performed by the removal of the signal's redundancy, and sometimes causes loss of information. A basic problem in waveform coding is to achieve the minimum possible distortion for a given encoding rate or, equivalently, to achieve a given acceptable level of distortion with the least possible encoding rate. The first stage of the analog signal coding process is sampling and quantization. The sampling is performed mostly according to the Nyquist criterion after

low-pass filtering the signal with an anti-aliasing filter. After sampling, the signal is time-discrete and amplitude-continuous. In order to represent the sampled signal digitally, one has to perform quantization — mapping the sampled signal's amplitudes from the continuous plane to the discrete plane. The quantization in this stage is usually fine quantization (many quantization levels) so one can treat the sampled signal as "almost" amplitude-continuous. At the second stage of the coding process, the redundancy of the signal is removed using appropriate coding techniques, such as Pulse Code Modulation(PCM), Differential Pulse Code Modulation(DPCM), Adaptive Differential Pulse Code Modulation(ADPCM), orthogonal transforms, entropy encoding, etc.

Typically, computerized medical signal processing systems acquires a large amount of data that is difficult to store and transmit [6]. It is very desirable to find a method of reducing the quantity of data without loss of important information. All data compression algorithms seek to minimize data storage by eliminating redundancy where possible. The compression ratio is defined as the ratio of the number of bits of the original signal to the number of bits stored in the compressed signal. A high compression ratio is desired, typically, but using this alone to compare data compression algorithms is not acceptable. Generally the bandwidth, sampling frequency, and precision of the original data affect the compression ratio [7]. A data compression algorithm must also represent the data with acceptable fidelity. In biomedical data compression, the clinical acceptability of the reconstructed signal has to be determined through visual inspection from a medical expert. The residual between the reconstructed signal and the original signal may also be measured by a

numerical measure. A lossless data compression algorithm produces zero residual, and the reconstructed signal exactly replicates the original signal. However, clinically acceptable quality is neither guaranteed by a low nonzero residual nor ruled out by a high numerical residual [8].

The criterion for testing performance of compression algorithms includes three components: compression ratio, reconstruction error and computational complexity. The compression ratio and the reconstruction error are usually dependent on each other and are used to create the rate-distortion function of the algorithm. The computational complexity component is part of the practical implementation consideration but it is not part of any theoretical measure.

2.2 ECG Data Compression

The electrocardiogram (ECG) is a graphic record of the changes in magnitude and direction of the electrical activity, or, more specifically, the electric current, that is generated by the depolarization and repolarization of the atria and ventricles. This electrical activity is readily detected by electrodes attached to the skin. But neither the electrical activity that results from the generation and transmission of electrical impulses which are too feeble to be detected by skin electrodes nor the mechanical contractions and relaxations of the atria and ventricles (which do not generate electrical activity) appear in the electrocardiogram. After the electric current generated by depolarization and repolarization of the atria and ventricles is detected by electrodes, it is amplified, displayed on an oscilloscope, recorded on ECG paper, or stored in memory.

Figure 2.1 shows the typical ECG signal with three indicated parts: P wave, QRS complex, and T wave. The P wave is the result of slow-moving depolarization (contraction) of the atria. This is a low-amplitude wave of 0.1-0.2 mV and duration of 60-120 ms. The wave of stimulus spreads rapidly from the apex of the heart upwards, causing rapid depolarization (contraction) of the ventricles. This results in the QRS complex of the ECG, a sharp biphasic or triphasic wave of about 1 mV amplitude and approximately 80-100 ms duration. Ventricular muscle cells have a relatively long action potential duration of 300-350 ms. The plateau part of action potential of about 100-120 ms after the QRS is known as the ST segment. The repolarization (relaxation) of the ventricles causes the slow T wave with an amplitude of 0.1-0.3 mV and duration of 100-120 ms. Between T and P waves, there is a relatively long plateau part of small amplitude known as TP segment [9].

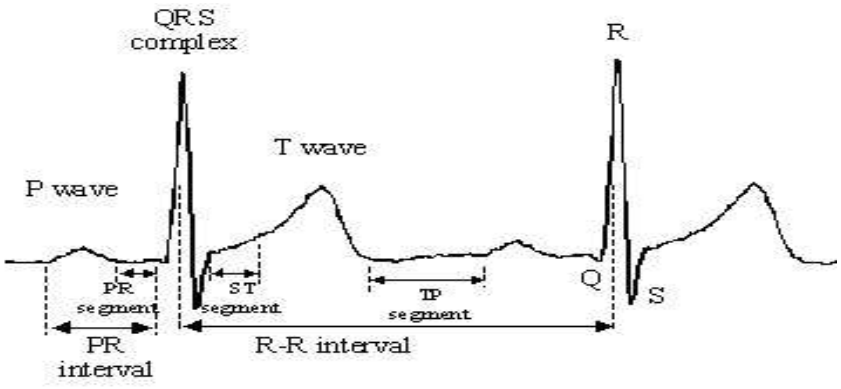

Figure 2.1: Typical ECG signal.

A large variety of techniques for ECG compression has been proposed and published over the last thirty years. These techniques have become essential in a large variety of applications, from diagnosis through supervision to monitoring ap-

plications. In general, compression techniques may be divided into two categories: lossless methods and methods that produce reconstruction errors. In most ECG applications, the errorless methods do not provide sufficient compression, and hence errors are to be expected in practical ECG compression systems. ECG compression methods have been mainly classified into three major categories [4, 7] : direct data compression, transformation methods, and parametric techniques. In the direct methods, the samples of the signal are directly handled to provide the compression. In the transformation methods, the original samples are subjected to a transformation and the compression is performed in the new domain. In the parametric methods, a preprocessor is employed to extract some features that are later used to reconstruct the signal. Most of the existing ECG data compression techniques lie in two of the three categories: the direct data and the transformation methods. Direct data compression techniques have shown a more efficient performance than the transformation techniques particularly in regard to processing speed and generally to compression ratio [7]. Although parametric methods usually have a greater computational complexity, algorithms that have recently joined this group, and are based on a beat codebook, seem to have the best compression performances [4, 10].

2.2.1 Distortion Measure in ECG Data Compression

One of the most difficult problems in ECG compression applications and reconstruction is defining the error criterion. The purpose of the compression system is to remove redundancy, the irrelevant information (which does not contain diagnostic information — in the ECG case). Consequently the error criterion has to

be defined such that it will measure the ability of the reconstructed signal to preserve the relevant information. In most ECG compression algorithms, the Percent Root-mean-square Difference (PRD) measure is employed:

$$PRD = \sqrt{\frac{\sum_{n=1}^{N}(x(n) - \tilde{x}(n))^2}{\sum_{n=1}^{N}(x(n) - \bar{x})^2}} \times 100 \tag{2.2.1}$$

where $x(n)$ is the original signal, $\tilde{x}(n)$ is the reconstructed signal, $\bar{x}$ is the mean of $x(n)$ and N is the length of the window over which the PRD is calculated. Sometimes in the literature, another definition is used, where the denominator is $\sum_{n=1}^{N} x(n)^2$, as given in Eq. (2.2.2):

$$PRD_2 = \sqrt{\frac{\sum_{n=1}^{N}(x(n) - \tilde{x}(n))^2}{\sum_{n=1}^{N}(x(n)^2)}} \times 100. \tag{2.2.2}$$

This second definition depends on the DC level of the original signal. If $x(n)$ contains a DC level, the PRD_2 will show irrelevant low results.

The two definitions as described in Eq.'s (2.2.1) and (2.2.2) are the same if the original signal has a zero mean. Since the first one is independent of the DC level of the original signal, it is more appropriate for use. There are some other error measures for comparing original and reconstructed ECG signals, such as the Root Mean Square error (RMS):

$$RMS = \sqrt{\frac{\sum_{n=1}^{N}(x(n) - \tilde{x}(n))^2}{N}} \tag{2.2.3}$$

or the signal-to-noise ratio (SNR), which is expressed as

$$SNR = 10 \log_{10} \left(\frac{\sum_{n=1}^{N}(x(n) - \bar{x})^2}{\sum_{n=1}^{N}(x(n) - \tilde{x}(n))^2} \right). \tag{2.2.4}$$

The relation between the SNR and the PRD is:

$$SNR = -20 \log_{10} PRD. \tag{2.2.5}$$

2.2.2 Compression Measure in ECG Data Compression

Many problems exist in the definition of compression measure. These problems mostly derive from the lack of uniformity (no standardization) in the test conditions of the various algorithms in respect of sampling frequencies and quantization levels. The size of compression is often measured by the Compression Ratio (CR) which is defined as the ratio between the bit rate of the original signal and the bit rate of the reconstructed one. In order to evaluate if the diagnostic information is well preserved in the reconstructed signal, such a criterion has been defined in the past as "diagnostic acceptability" [11]. Today the accepted way to examine diagnostic acceptability is to get cardiologists' evaluations of the system's performance. This solution is good for getting evaluations of coders' performances, but it can not be used as a tool for designing ECG coders and certainly, can not be used as an integral part of the compression algorithm. However, in order to use such a criterion for coders design, one has to give it a mathematical model. As yet, there is no such mathematical structure to this criterion, and all accepted error measures are still variations of the Mean Square Error or absolute error, which are easy to compute mathematically, but are not always diagnostically relevant.

The problem is that every algorithm is fed with an ECG signal that has a different sampling frequency and a different number of quantization levels; thus, the bit rate of the original signal is not standard. Some attempts were made in the past to define standards for sampling frequency and quantization, but these standards were not implemented and the algorithms' developers still use rates and quantizers

that are convenient to them. In the literature, some authors use the number of bits transmitted per sample of the compressed signal as a measure of information rate. This measure removes the dependency on the quantizer resolution, but the dependence on the sampling frequency remains. Another way is using the number of bits transmitted per second. This measure removes the dependence on the quantizer resolution as well as the dependence on the sampling frequency.

In the following sections, we will give an overview of conventional ECG data compression techniques.

2.3 Direct Data Compression Methods

Direct data compression methods rely on prediction or interpolation algorithms which try to diminish redundancy in a sequence of data by looking at successive neighboring samples. Prediction algorithms employ a *priori* knowledge of previous samples, whereas interpolation algorithms use a *priori* knowledge of both previous and future samples. In consideration of the algorithmic structure of present ECG data reduction methods, direct data compression schemes can be classified into three categories: tolerance-comparison data compression methods, data compression by a differential pulse code modulation (DPCM) techniques, and entropy coding techniques. In the first category, a preset error threshold is utilized to discard data samples; the higher the preset error threshold the higher the data compression ratio with result in a lower recovered signal fidelity. The DPCM techniques attempt to diminish signal redundancy by using intersample correlation. The entropy coding techniques reduce signal redundancy whenever the quantized signal amplitudes have

a nonuniform probability distribution.

2.3.1 Tolerance-Comparison Data Compression Techniques

Most of the tolerance-comparison data compression techniques employ polynomial predictors and interpolators. The basic idea behind polynomial prediction or interpolation compressors is to eliminate samples, from a given data set, which can be implied by examining preceding and succeeding samples. The implementation of such compression algorithms is usually executed by setting a preset error threshold centered around an actual sample point. Whenever the difference between that sample and a succeeding future sample exceeds the preset error threshold, the data between the two samples is approximated by a line whereby only the line parameters (e.g., length and amplitude) are saved. In this section, some of the known tolerance-comparison ECG compression algorithms will be introduced.

1. **The Amplitude Zone Time Epoch Coding (AZTEC) Technique**

   The AZTEC algorithm was originally developed by Cox *et al.* [12] for preprocessing real-time ECG's for rhythm analysis. It has become a popular data reduction algorithm for ECG monitors and databases with an achieved compression ratio of 10:1 (500 Hz sampled ECG with 12 bit resolution). However, the reconstructed signal demonstrates significant discontinuities and distortion (PRD of about 28%). In particular, most of the signal distortion occurs in the reconstruction of the P and T waves due to their slowly varying slopes. The AZTEC algorithm converts raw ECG sample points into plateaus and slopes. The AZTEC plateaus (horizontal lines) are produced by utilizing the

zero-order interpolation. The stored values for each plateau are the amplitude value of the line and its length (the number of samples with which the line can be interpolated within aperture). The production of an AZTEC slope starts when the number of samples needed to form a plateau is less than three. The slope is saved whenever a plateau of three samples or more can be formed. The stored value of the slope are the duration (number of samples of the slope) and the final elevation (amplitude of last sample point). Even though the AZTEC provides a high data reduction ratio, the reconstructed signal has poor fidelity mainly because of the discontinuity (step-like quantization) of the waves. A significant improvement in the shape, while smoothing the discontinuity, is achieved by using a smoothing filter, but this improvement causes higher error. A modified AZTEC algorithm was proposed in [13], in which the threshold is not a constant but a function of the temporary changes in the signal properties. A data compression ratio comparable to that of the original AZTEC algorithm was achieved and signal reconstruction was improved (by means of PRD). In another algorithm [14], vector quantization was used along with the m-AZTEC to produce a multi-lead ECG data compressor. This approach yieldes a compression ratio of 8.6 : 1.

2. **The Turning Point Technique**

The turning point (TP) data reduction algorithm [15] was developed for the purpose of reducing the sampling frequency of an ECG signal from 200 to 100 Hz without diminishing the elevation of large amplitude QRS's. The algorithm processes three data points at a time: a reference point $x(i)$ and

two consecutive data points $x(i+1)$ and $x(i+2)$. Either $x(i+1)$ or $x(i+2)$ is to be retained. This depends on which point preserves the slope of the original three points. In this method, only the amplitudes are to be stored but not their locations. The TP algorithm produces a fixed compression ratio of $2:1$ whereby the reconstructed signal resembles the original signal with some distortion.

3. **The Coordinate Reduction Time Encoding System (CORTES) Scheme**

   The CORTES algorithm [6] is a hybrid of the AZTEC and TP algorithms. In this algorithm, the ability of the TP is exploited to track the fast changes in the signal, and the ability of the AZTEC is exploited to compress effectively isoelectric regions. CORTES applies the TP algorithm to the high frequency regions (QRS complexes), whereas it applies the AZTEC algorithm to the lower frequency regions and to the isoelectric regions of the ECG signal. For signals sampled at 200 Hz with 12 bit resolution, the compression ratio is $5:1$ with a PRD of 7% .

4. **Fan and SAPA Techniques**

   Fan and Scan-Along Polygonal Approximation (SAPA) algorithms, are both based on first-order interpolation [7]. The Fan algorithm was tested on ECG signals in the 1960's by Gardenhire, and further description was given in a report [16] of the Fan Method. In this method, the compressor searches for the most distant sample (on the time axis), such that if a line is drawn between it and the last stored sample, the local error along the line will be lower than a specific error tolerance. The location and the amplitude of this sample

are stored, and this process recurs. The reconstructed signal looks like a broken line, and its fidelity depends on the error threshold. The greater the threshold is, the better the compression ratio, and the poorer the fidelity. The Scan-Along Polygonal Approximation (SAPA) techniques [17] are based on a similar idea to the Fan algorithm, and have similar performances. The SAPA2 algorithm, one of the three SAPA algorithms, showed the best results. For signals sampled at 250 Hz with 12 bit resolution, the compression ratio is $3:1$ with a PRD of 4%.

5. **The Slope Adaptive Interpolation Encoding Scheme (SAIES)**

   The SAIES algorithm [18] combines the AZTEC and Fan compression techniques. It employs the AZTEC's slope compression technique in encoding the QRS-complex, and utilizes the Fan technique for encoding the low-frequency waves of the ECG (the isoelectric, P, and T waves). For signals sampled at 166 Hz with 10 bit resolution, the compression ratio is $5.9:1$ with a PRD of 16.3%.

6. **The SLOPE Algorithm**

   The basic idea of SLOPE is repeatedly delimiting linear segments. In the work of [19], the algorithm attempts to delimit linear segments of different lengths and different slopes in the ECG signal. It considers some adjacent samples as a vector, and this vector is extended if the coming samples falls within a fan spanned by this vector and a threshold angle; otherwise, it is delimited as a linear segment. Similar to the SAPA and Fan algorithms, the reconstructed signal looks like a broken line. For signals sampled at 120 Hz

Table 2.1: Performance of the Tolerance-Comparison Data Compression Techniques for ECG signal

Method	AZTEC	TP	CORTES	SAPA	SAIES	SLOPE
CR	10	2	5	3	5.9	5.5
PRD(%)	28	-	7	4	16.3	-

with 8 bit resolution, the compression result is an average bit rate of 190 bps while still maintaining clinically significant information.

Table 2.1 summarizes the performance of the Tolerance-Comparison Data Compression Techniques.

2.3.2 Data Compression by Differential Pulse Code Modulation (DPCM)

The Pulse Code Modulation (PCM) is the earliest, the simplest, and the most popular coder in digital coding systems of signals. A PCM coder is nothing more than a waveform sampler followed by an amplitude quantizer. In PCM, each sample of the waveform is encoded independently of all the others. However, most source signals sampled at the Nyquist rate or faster exhibit significant correlation between successive samples. In other words, the average change in amplitude between successive samples is relatively small. Consequently, an encoding scheme that exploits the redundancy in the samples will result in a lower bit rate for the source output. A relatively simple solution is to encode the differences between successive samples rather than the samples themselves. Since differences between samples are expected to be smaller than the actual sampled amplitudes, fewer bits are required to represent the differences.

Some algorithms for ECG compression based on DPCM have been presented in the literature. Some of them use the DPCM as minor part of the whole compression scheme. The basic idea behind the DPCM is that the residual between the actual sample $x(n)$ and the estimated sample value $\hat{x}(n)$ defined by:

$$r(n) = x(n) - \hat{x}(n). \tag{2.3.6}$$

is quantized and transmitted or stored. The reconstruction error is mainly caused by the amplitude quantization noise of the quantized residual. The performances of DPCM coders as linear predictors for a compression system for ECG signals were tested [20]. Some important conclusions were reached: increasing the predictor order beyond 2 does not improve performance and the prediction coefficients are barely changed as a function of time and, therefore, there is no use of Adaptive DPCM (ADPCM). Huffman coding was combined with this compressor, and the reported performances were not significantly different from the performances of other direct compression methods. For signals sampled at 500 Hz with 8 bit resolution, the compression ratio is about $7.8:1$ with a PRD of 3.5%.

In [1], an attempt was made to exploit the quasi-periodic characteristic of the ECG signal to reduce the variance of the prediction error. The algorithm processes every cycle (beat) of the heart separately with two-stage DPCM. In the first stage, the prediction error (residual) of the current heartbeat is calculated by DPCM with a third order linear predictor. In the second stage, the residual of the previous beat is subtracted from the residual of the current one, and the difference is encoded by entropy coding. Figure 2.2 illustrates this compression scheme. A compression ratio of $2:1$ without any reconstruction error is achieved. Another important work

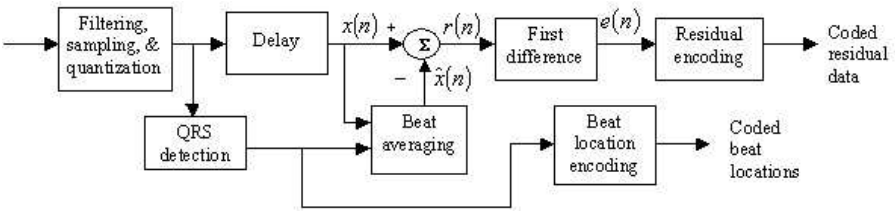

Figure 2.2: Compression by two-step DPCM [1].

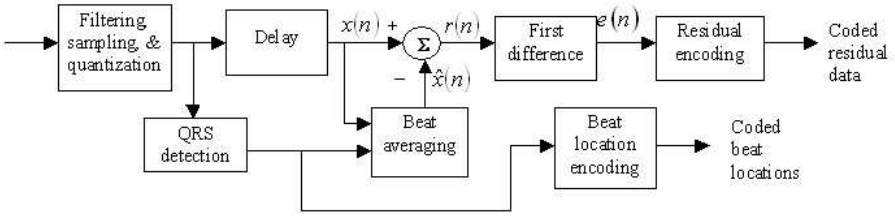

Figure 2.3: Compression by average beat subtraction [2].

is [2], in which the current heartbeat is subtracted from an average beat, the residual is first differenced and then Huffman encoded, see Figure 2.3. Using quantization step sizes of $35\mu V$ and a sampling frequency of 100 Hz, the compressor is reported to produce an average data rate of 174 bps for the 24 hour MIT-BIH arrhythmia database [21].

2.3.3 Entropy Coding

A Discrete Memoryless Source (DMS) coding system produces a symbol every τ_s seconds. Each symbol is selected from a finite alphabet of symbols x_i; $i = 0, \ldots, L$, occurring with probabilities $p(x_i), i = 1, 2, \ldots, L$. The entropy of the DMS in bits per source symbol is

$$H(X) = -\sum_{i=1}^{L} p(x_i) \log_2 p(x_i) \leqslant \log_2 L \tag{2.3.7}$$

where equality holds when the symbols are equally probable. The average number of bits per source symbol is $H(X)$ and the source rate in bits per second is defined as

$$R = \frac{H(X)}{\tau_s}. \tag{2.3.8}$$

In a coder that fits one set of N bits for every symbol (fixed-length codewords), the number of bits required for symbol coding is

$$N = \lceil \log_2 L \rceil. \tag{2.3.9}$$

When the source symbols are not equally probable, a more efficient encoding method is to use variable-length codewords. An example of such encoding is the Morse code. In the Morse code, the letters that occur more frequently are assigned short codewords and those that occur infrequently are assigned long codewords. Following this general philosophy, we may use the probabilities of occurrence of the different source letters in the selection of the codewords. The problem is to devise a method for selecting and assigning the codewords to source letters. This type of encoding is called entropy coding.

Entropy coding such as Huffman coding [22] has been implemented as part of some ECG DPCM coders and other coders. In the DPCM coders, like those discussed in Section 2.3.2, the residual was mapped into variable length codewords instead of fixed length ones. The residual in those DPCM coders, has a non-uniform distribution and therefore, a better compression ratio could be achieved.

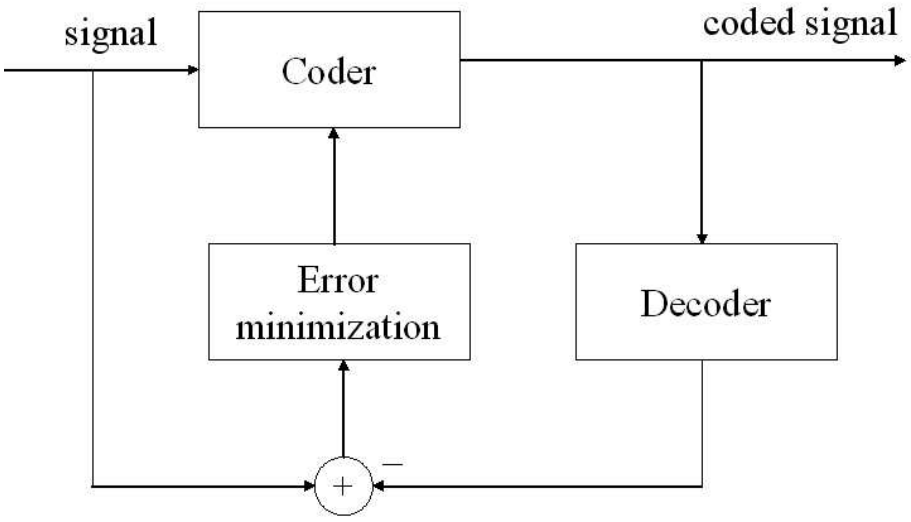

Figure 2.4: Simplied representation of an analysis by synthesis coder [3].

2.3.4 Analysis by Synthesis Coding

The principle of an analysis-by-synthesis coder [3] is illustrated in Figure 2.4. The transmitter (encoder) incorporates a decoding structure similar to that used at the decoder. For each quantized parameter configuration, an error criterion comparing the original and the reconstructed signal is computed. Usually this criterion is the mean-squared error (or a variation of it) computed as the difference between the original and the reconstructed signals. The criterion is then used to select the best configuration of the quantized coder parameters and the index or the indices corresponding to this parameter configuration are transmitted to the receiver. The receiver uses the same decoding structure to reconstruct the original signal. In the work of [23], analysis by synthesis coding has been used in ECG signal processing.

2.4 Transformation Methods

Transformation techniques have generally been used in vector cardiography or multi-lead ECG compression and require preprocessing of the input signal by a linear orthogonal transformation and encoding of the output (expansion coefficients) using an appropriate error criterion. For signal reconstruction, an inverse transformation is carried out and the ECG signal is recovered with some error. In principle, if the samples' sequence of the current ECG beat is considered as an N-dimensional vector $\mathbf{x}$, the transform of $\mathbf{x}$ is given by the N-dimensional vector $\mathbf{y}$:

$$\mathbf{y} = \mathbf{A}\mathbf{x} \tag{2.4.10}$$

where $\mathbf{A}$ is the transform matrix ($N \times N$). The original signal $\mathbf{x}$ can be obtained from the transform vector by the inverse transform:

$$\mathbf{x} = \mathbf{A^{-1}}\mathbf{y}, \tag{2.4.11}$$

where for the class of orthogonal transforms [24], we have

$$\mathbf{A^{-1}} = \mathbf{A^{T}}. \tag{2.4.12}$$

Assuming $\mathbf{A}$ is not singular, the column vectors of $\mathbf{A^{-1}}$ can be related as the basis vectors, and $\mathbf{x}$ as linear combination of the basis vectors, where the elements of $\mathbf{y}$ are the combination coefficients. The compression is performed by appropriate bit allocation to every element of $\mathbf{y}$, where the goal is minimization of the general amount of bits for a given error level. Many orthogonal transform compression algorithms for ECG signals have been presented in the last thirty years, such as the

Fourier Transform [25], Walsh Transform [26], Cosine Transform [Ahmed, Milne, and Harris, 1975], and Karhunen-Loeve Transform (KLT) [27]. The typical performances of the transform methods are compression ratio between 3 : 1 to 12 : 1, where the KLT has the best compression ratio. The KLT is an optimal transform in the sense that the least orthonormal functions are required to represent the signal. In the recent years, since the Wavelet Transform (WT) was introduced [28], many ECG compression algorithms based on the Wavelet Transform have been proposed [29,30]. A compression ratio from 13.5 : 1 to 31.5 : 1 with the corresponding PRDs between 1.9% and 13% is achieved.

2.5 Parametric Methods

Although many of the reported ECG compression algorithms fall into the above two categories, more and more ECG compression algorithms based on parametric techniques have been proposed in recent years. Some of these algorithms are hybrids of direct and parametric techniques or transformation and parametric techniques. The compression algorithms based on parametric techniques require a preprocessing stage, which is sometimes heavy in the sense of calculation, but this is not a problem for computers today.

1. **Beat Codebook**

   In the recent years, many ECG compression algorithms based on a Beat Codebook have been presented. This group of algorithms is very efficient in ECG compression because it exploits the quasi-periodic nature of ECG signals. In

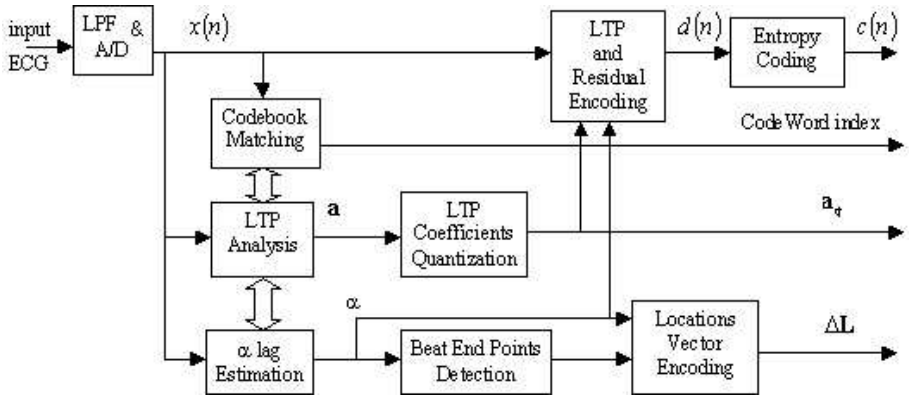

Figure 2.5: ECG compression based on long term prediction [4].

this method, the redundancy, which exists in the form of correlation between beats (complexes) [31, 32], is reduced by matching a beat from a beat codebook to the currently processing beat. All algorithms belonging to this group have a QRS detector stage to locate and segment every beat. In the work of [33], average-beat templates are subtracted from the ECG signal. The residual (which has reduced variance) is quantized adaptively, first differenced, and Huffman encoded. The coded residual signal is stored along with the beat type (two bits) and the beat arrival time, as illustrated in Figure 2.5. This compression algorithm was tested with the MIT-BIH database, and the achieved bit rate was 193.3 bps, with PRD between 4.33% and 19.3%, depending on the tested signal. Nave *et al.* [4] used a Long-Term Prediction (LTP) model, where the prediction of the nth sample is made using samples of past beats. The LTP residual signal was quantized and further compressed using the Huffman coding. The compression ratio depends on the number of the residual quantizer levels, which is determined prior to compression execution. For each cycle (beat) a number of parameters are to be stored (transmitted): the index of

the chosen beat codeword, the quantized LTP coefficients, the beat locations vector, the quantizer range, and the coded residual (optionally). The algorithm was tested on a local ECG database, which has a sampling frequency of 250 Hz and quantization of 10 bits/sample. Bit rates between 71 bps and 650 bps with PRDs between 10% and 1% were achieved.

2. **Artificial Neural Network (ANN)**

   Some ECG compression algorithms based on Artificial Neural Network have been presented since 1989. Iwata *et al.* [34] used dual three-layered neural networks which are composed of 70 units of input layer, a few units in the hidden layer, and 70 units in the output layer. One network is used for data compression and another is used for learning with current signals. The compressed signal contains the interconnecting weights of the network and the activation levels of hidden units for every consecutive heart beat. The ECG signal is reconstructed at the activation levels of the output units. Another work [5] was based on a similar idea, and used three layers: input, hidden, and output layer. The hidden layer had a reduced number of nodes to produce compression (see Figure 2.6). The compression ratio is controlled by the ratio of hidden-layer neurons to input- and output-layer neurons. Fewer hidden neurons produce higher compression ratios and poorer reconstruction errors. Bit rates between 304 bps and 64 bps with PRDs between 4.6% and 6.1% were achieved when using mean waveform and DC removal in the algorithm.

3. **Peak Picking**

   The peak-picking compression techniques are generally based on the sampling

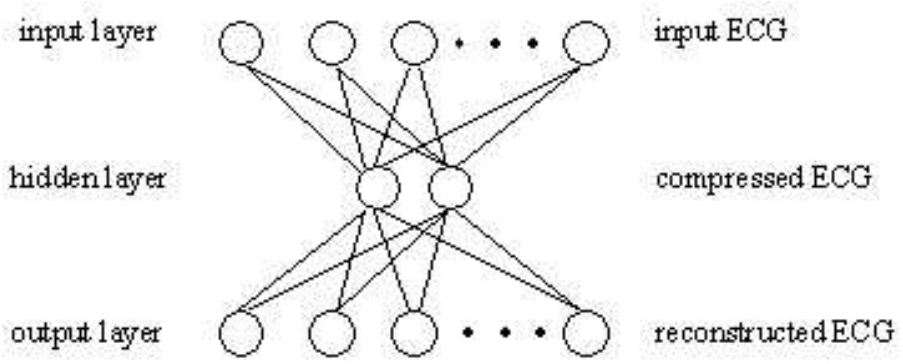

Figure 2.6: ECG compression by ANN [5].

of a continuous signal at peaks (maxima and minima) and other significant points of the signal [7]. The basic operation involves the extraction of signal parameters that convey most of the signal information. These parameters include the amplitude and location of the maxima and the minima points, slope changes, zero-crossing intervals, and points of inflection in the signal. These parameters are substituted in place of the original signal. The signal is reconstructed by polynomial fitting techniques such as parabolic functions.

4. **Beat Codebook**

In the recent years, many ECG compression algorithms based on a Beat Codebook have been presented. This group of algorithms is found to be very efficient in ECG compression because it exploits the quasi-periodic nature of ECG signals. In this method, the redundancy, which exists in the form of correlation between beats (complexes), is reduced by matching a beat from a beat codebook to the currently processed beat. All algorithms belong to this group have a QRS detector stage to locate and segment every beat.

Table 2.2: Comparison of performance of some existing ECG data compression techniques

Category	Method	CR	PRD (%)
Direct Data Compression Methods	AZTEC	10	28
	CORTES	5	7
	SAPA	3	4
	SAIES	5.9	16.3
	DPCM	7.8	3.5
Transformation Methods	WT	13.5–31.5	1.9–13
Parametric Methods	Beat Codebook	3.8–35.2	1–10
	ANN	8.2–39	4.6–6.1

To summarize, Table 2.2 shows the compression ration (CR) and percentage root-mean-square distortion (PRD) performance of different conventional methods for ECG data compression. From this table, it is easy to see that, the transformation methods and parametric methods performs better than direct compression methods in yielding high compression ratio with low distortion. Since in ECG compression and reconstruction, the most important factor is to preserve the diagnostic information, in our methods, we will also evaluate if the morphology of the signal can be preserved or not.

Chapter 3

A Novel Wavelet-based Pattern Matching Method

In this chapter, firstly, we will give an introduction to the wavelet transform; then we will discuss the compression and reconstruction scheme step by step; finally, we will give the experimental results of this wavelet-based pattern matching (WBPM) algorithm. In our study, we take advantage of the interbeat correlation across heartbeats to achieve efficient ECG data compression.

3.1 Wavelet Transform

The main idea behind wavelet analysis is to decompose a signal f into a basis of functions Ψ_i:

$$f = \sum_i a_i \Psi_i. \tag{3.1.1}$$

To have an efficient representation of the signal f using only a few coefficients a_i, it is very important to use a suitable family of functions Ψ_i. The functions Ψ_i should match the features of the data we want to represent.

Real-world signals usually have the following feature: limited in both time domain (time-limited) and frequency domain (band-limited). Time-limited signals can be represented efficiently using a basis of block functions (Dirac delta functions for infinitesimal small blocks), but block signals are not limited in frequency. Band-limited signals can be represented efficiently using a Fourier basis, but sines and cosines are not limited in time domain.

What we need is a trade off between the pure time-limited and band-limited basis functions, a compromise that combines the best of both worlds: wavelets (small waves).

Historically, the concept of "ondelettes"or "wavelets" started to appear more frequently only in the early 1980's. This new concept can be viewed as a synthesis of various ideas originating from different disciplines including mathematics, physics and engineering. In 1982, Jean Morlet, a French geophysical engineer, discovered the idea of the wavelet transform, providing a new mathematical tool for seismic wave analysis. In Morlet's analysis, signals consist of different features in time and frequency, but their high-frequency components would have shorter time duration than their low-frequency components. In order to achieve good time resolution for the high-frequency transients and good frequency resolution for the low-frequency components, Morlet first introduced the idea of wavelets as a family of functions constructed from translation and dilations of a single function called the *"mother wavelet"* $\Psi(t)$. They are defined by

$$\Psi_{a,b}(t) = \frac{1}{\sqrt{|a|}}\Psi\left(\frac{t-b}{a}\right), \qquad a, b \in \mathbb{R}, a \neq 0, \tag{3.1.2}$$

where a is called a *scaling parameter* which measures the degree of compression or scale, and b a *translation parameter* which determines the time location of the wavelet. If $|a| < 1$, the wavelet given in Eq. (3.1.2) is the compressed version (smaller support in time-domain) of the mother wavelet and corresponds mainly to higher frequencies. On the other hand, when $|a| > 1$, $\Psi_{a,b}(t)$ has a larger time-width than $\Psi(t)$ and corresponds to lower frequencies. Thus, wavelets have time-width adapted to their frequencies. This is the main reason for the success of the Morlet wavelets in signal processing and time-frequency signal analysis. It may be noted that the resolution of wavelets at different scales varies in the time and frequency domains as governed by the Heisenberg uncertainty principle. At large scale, the solution is coarse in the time domain and fine in the frequency domain. As the scale a decreases, the resolution in the time domain becomes finer while that in the frequency domain becomes coarser.

The calculation of discrete wavelet transform and its inverse is fast and stable. Furthermore, one of the main features of wavelets is their good decorrelation:

- Wavelets are localized in both the space/time and scale/frequency domains. Hence they can easily detect local features in a signal.
- Wavelets are based on a multi-resolution analysis. A wavelet decomposition allows to analyze a signal at different resolution levels (scales).
- Wavelets are smooth, which can be characterized by their number of vanishing moments. A function defined on the interval $[a, b]$ has n vanishing moments if

$$\int_a^b f(x)x^i dx = 0, \qquad \forall i = 0, 1, \cdots, n-1. \tag{3.1.3}$$

The higher the number of vanishing moments, the better smooth signals can be approximated by a wavelet basis.

In the past few years, researchers in applied mathematics and signal processing have developed powerful wavelet methods for the multiscale representation and analysis of signals. These new tools differ from the traditional Fourier techniques by the way in which they localize the information in the time-frequency plane; in particular, they are capable of trading one type of resolution for the other, which makes them especially suitable for the analysis of nonstationary signals. One privileged area of applications where these properties have been found to be relevant is biomedical engineering. The main difficulty in dealing with biomedical objects is the extreme variability of the signals and the necessity to operate on a case by case basis. Often one does not know a *priori* what is the pertinent information and/or at which scale it is located. For example, it is frequently the deviation of some signal feature from the normal that is the most relevant information for diagnosis. As a result, the problems tend to be less well defined than those in engineering and the emphasis is more on designing robust methods that work in most circumstances, rather than procedures that are optimal under very specific assumptions. Another important aspect of biomedical signals is that the information of interest is often a combination of features that are well localized temporarily or spatially and others are more diffuse. This requires the use of analysis methods sufficiently versatile to handle events that can be at opposite extremes in terms of their time-frequency localization. In essence, the wavelet transform (WT) performs a correlation analysis, which is the basis for the matched filter, and can be utilized for QRS complex

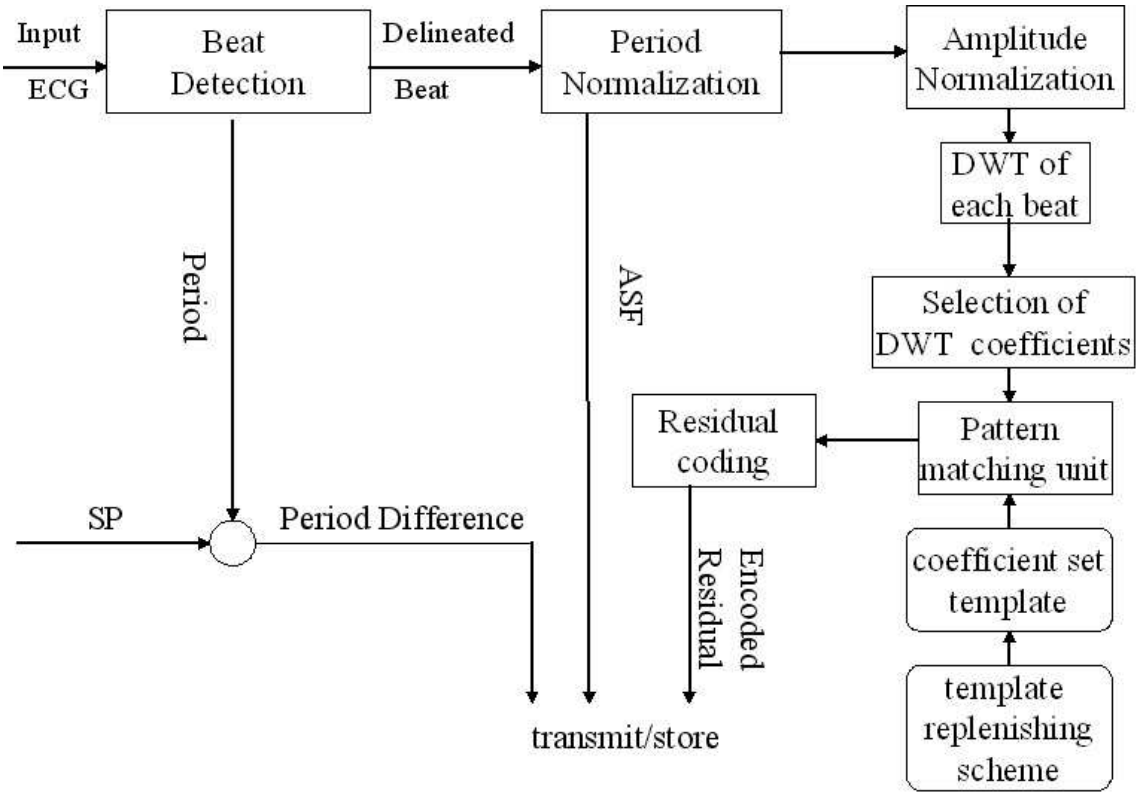

Figure 3.1: Block schematic of the encoder.

detection in ECG signals. Moreover, data compression can be achieved by quantization in wavelet domain, or by simply discarding certain insignificant coefficients. In our study, we take advantage of these characteristics of wavelets to achieve efficient ECG data compression.

The encoding procedures will be discussed step by step in the following sections. The block schematic for the encoder of the novel wavelet-based pattern matching (WBPM) method is shown in Figure 3.1.

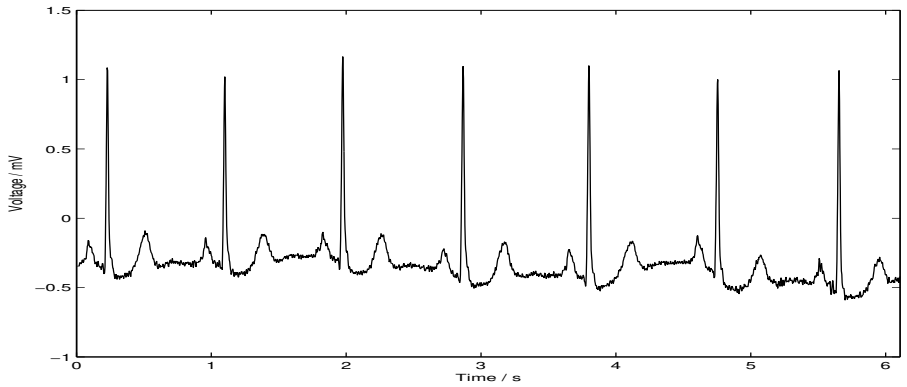

Figure 3.2: Typical waveform of ECG.

3.2 Beat Normalization

The waveform of a typical ECG, as shown in Figure 3.2 (record 101 from the MIT-BIH Arrhythmia Database [21]), demonstrates that an ECG signal is intrinsically composed of a sequence of beats with similar pattern. In order to explore the correlation between consecutive beats, first we have to normalize the signal to eliminate heart rate variability.

3.2.1 Period Normalization

For delineating cycles, we define a cycle as the signal from one R-peak to the next. We use the technique reported in [35] for QRS detection. Multirate techniques [36] is utilized for normalizing the period of each isolated beat. This involves sampling rate changing by different fractional factors for different cycles and converts the beats of different periods into beats of a constant period, thus eliminating the effect of heart rate variability. The fixed length of the cycles is selected based on the maximum possible period of any cardiac cycle and sampling frequency. The modified sampling

rate must still satisfy the Nyquist criterion. We have selected a length such that the new sampling rate is always higher than the original one, ensuring that there will be no distortion of the signal. The standard period (SP) is estimated from some initial cycles of the data being coded, and this value is initially sent to the decoder. During encoding, the difference between the actual period of a cycle and the standard period is transmitted.

To perform period normalization, we first interpolate the variable period beat vectors by a factor L, which is the fixed period planned for. Then the signal is downsampled by the appropriate factor for each cycle, so that the length of all cycles become uniform. In our case, only the interpolation filter and downsampling are required. Since ECG signal has been interpolated by a sufficiently high value, no error occurs in downsampling. The details of implementation are given below.

If $x(n)$ is the input to an interpolation filter with an upsampling factor L and an impulse response $h(n)$, then the output $y(n)$ is given by

$$y(n) = \sum_{k=\infty}^{\infty} x(k)h(n - kL). \tag{3.2.4}$$

The upsampler simply inserts $L - 1$ zeros between successive samples. The filter $h(n)$, which operates at a rate L times higher than that of the input signal, replaces the inserted zeros with interpolated values. Polyphase implementation of this filter [36] ensures efficient interpolation. The output $y(n)$ of a decimation filter, with an impulse response $h(n)$ and a downsampling factor M, where $M < L$, is given by

$$y(n) = \sum_{k=\infty}^{\infty} x(k)h(nM - k) \tag{3.2.5}$$

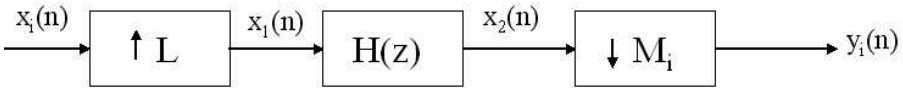

Figure 3.3: Period normalization.

where $h(n)$ is a lowpass filter used to remove the aliasing caused by the downsampling of the signal. In case the signal does not contain frequencies above π/M, there is no need for the decimation filter; downsampling alone will do. The change of sampling rate thus achieved is a reversible process, provided Nyquist condition is satisfied; if the resampled beat is brought back to the original sampling rate by multirate processing, there will be no distortion. The output of our system is given by

$$y_i(n) = \sum_{k=0}^{P_i-1} x_i(k)h(nM_i - kL) \tag{3.2.6}$$

where $x_i(n)$, $y_i(n)$ are the nth samples of the ith input beat and period normalized beat, respectively, $h(n)$ is the impulse response of the filter, P_i is the total number of samples in ith original beat, and L, M_i are, respectively, the upsampling and downsampling factors for the ith beat vector. The block schematic for this operation is shown in Figure 3.3. The interpolation is efficiently accomplished in multiple stages.

3.2.2 Amplitude Normalization

Amplitude normalization brings about further similarity between the beat patterns. Each sample of a beat is divided by the magnitude of the largest sample of the beat, the largest magnitude is defined as the amplitude scale factor (ASF). This makes the magnitude the largest sample(s) of each beat equal to unity. Thus, the variations

between the magnitudes of different cycles are minimized. Figure 3.4 shows that the period and the amplitude normalization do not introduce any distortion in the signal and also demonstrates its efficacy in enhancing the interbeat correlation. For each cycle being coded, the amplitude scale factor (ASF) is transmitted to the decoder.

3.3 Wavelet-based Pattern Matching of Normalized Beats

3.3.1 Wavelet Transform of Normalized Beats

In wavelet analysis, a mother wavelet function $\Psi(x)$ and a linear combination of its dilated and/or shifted versions are used to represent a given signal

$$f(x) = \sum_{j\in\mathbb{Z}} \sum_{k\in\mathbb{Z}} w_{j,k}\Psi_{j,k}(x) \tag{3.3.7}$$

where $f(x)$ is the signal to be analyzed, $\Psi_{j,k}(x)$ is the dilated and shifted version of the mother wavelet $\Psi(x)$, j and k determine the dilation and shift factor respectively, $w_{j,k}$ are the wavelet coefficients, and

$$\Psi_{j,k}(x) = \Psi(2^j x - k). \tag{3.3.8}$$

It is desired that the wavelet basis functions be orthonormal in order to simplify the computation of the coefficients [29]. From Eq. (3.3.7) and the orthonormality of basis functions, we get the wavelet coefficients $w_{j,k}$ as

$$w_{j,k} = \langle f(x), \Psi_{j,k}(x)\rangle = \int_{-\infty}^{\infty} f(x)\Psi_{j,k}(x)dx. \tag{3.3.9}$$

From Eq.'s (3.3.7) and (3.3.8) we get

$$f(x) = \sum_{j\in\mathbb{Z}} \sum_{k\in\mathbb{Z}} w_{j,k}\Psi(2^j x - k). \tag{3.3.10}$$

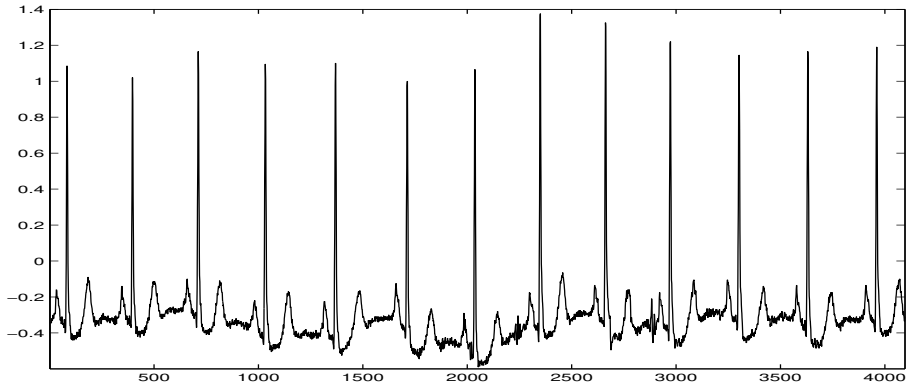

(a)

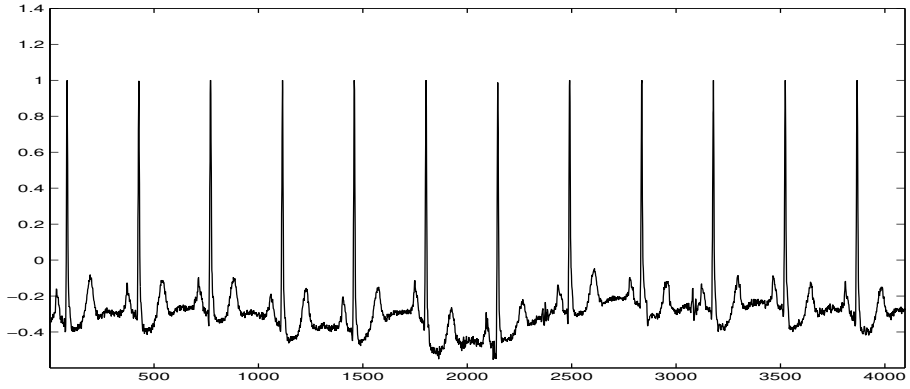

(b)

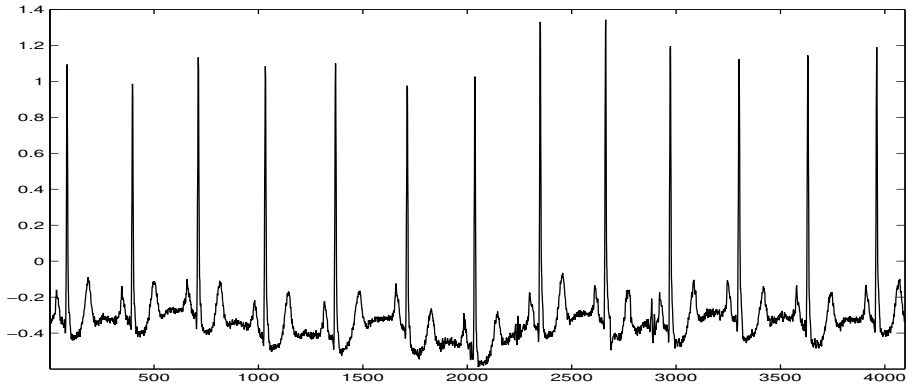

(c)

Figure 3.4: Signal normalization and reconstruction: (a) original signal; (b) normalized signal; and (c) reconstructed signal. The vertical axis represents the amplitude and the horizontal axis represents the sample index.

While setting up a discrete wavelet transform algorithm, it is convenient to limit the range of the independent variable x to one unit interval so that $f(x)$ is defined only for $x \in [0, 1]$. Here, x is a nondimensional variable; so if the independent variable is the time t, and we are interested in a signal over duration T, then $x = t/T$.

Of the many available orthogonal basis functions $\Psi_{j,k}(x) \in \mathbf{L}^2(\mathbf{R})$, we have used Daubechies-4 (D4) functions for representing each normalized beat. The D4 wavelet $\Psi_{0,0}(x)$ occupies three unit intervals $x \in [0, 3]$. The expansion of $f(x)$ in $x \in [0, 1]$ can be written as

$$\begin{aligned} f(x) = w_{01}\phi(x) + w_{11}\Psi(x) + [w_{21}\ w_{22}] \begin{bmatrix} \Psi(2x) \\ \Psi(2x-1) \end{bmatrix} \\ + [w_{31}\ w_{32}\ w_{33}\ w_{34}] \begin{bmatrix} \Psi(4x) \\ \Psi(4x-1) \\ \Psi(4x-2) \\ \Psi(4x-3) \end{bmatrix} + \cdots \end{aligned} \tag{3.3.11}$$

where $\phi(x) = 1, x \in [0, 1]$ and w_{jk} refers to the wavelet coefficient at scale j and location k. Let us form a vector X by stacking the wavelet coefficients at scale 0,1,2, ..., 7 as defined below

$$X = [w_{01}\ w_{11}\ w_{21}\ w_{22}\ w_{31}\ w_{32}\ w_{33}\ w_{34}\ \cdots]. \tag{3.3.12}$$

Then from Eq.'s (3.3.11) and (3.3.12) we get

$$\begin{aligned} f(x) = X(0)\phi(x) + X(1)\Psi(x) + [X(2)\ X(3)] \begin{bmatrix} \Psi(2x) \\ \Psi(2x-1) \end{bmatrix} \\ + [X(4)\ X(5)\ X(6)\ X(7)] \begin{bmatrix} \Psi(4x) \\ \Psi(4x-1) \\ \Psi(4x-2) \\ \Psi(4x-3) \end{bmatrix} \\ + \cdots + X(2^j + k)\Psi(2^j x - k) \end{aligned} \tag{3.3.13}$$

where $X(n)$ is the nth element of the vector X.

Because of the high suitability of time-localized basis functions for representing the locally nonstationary ECG cycle, not all the wavelet coefficients are significant in the reconstruction of any beat. By choosing a fixed set of significant coefficients to be transmitted from each beat, important rhythm and morphological information can still be retained. Normalized beats enable us to achieve this end.

3.3.2 Pattern Matching of DWT Coefficients

Since there is a definite correlation between the corresponding wavelet coefficients of different normalized beats, the current one can be approximated by certain past coefficients, and only the residual needs to be transmitted. In our study, we perform pattern matching of wavelet coefficients across beats. The variance of the residuals obtained is less than that of the original coefficients. Thus, we are able to allocate less bits to each residual than the number of bits required for each wavelet coefficient set.

After performing the wavelet transform on each normalized beat, a pattern matching process is then performed. In this stage, a *coefficient set template pattern library* of size $N_p = 1$, which contains only one pre-selected set of wavelet coefficients, is designed. The coefficient set template pattern is a pattern appropriately selected from the wavelet coefficients of the data file to be coded and needs to be distortionlessly transmitted to the decoder initially so that the coefficient set template pattern library in the decoder has the same coefficient set as in the encoder. A simple template replenishing scheme for synchronously updating the libraries in the encoder and the decoder is adopted. Whenever the wavelet coefficient set of input

beat varies drastically and becomes very dissimilar from the one in the library during the encoding session, the library must be updated by replacing it with the input coefficient set. The new coefficient set template pattern must also be distortionlessly transmitted to the decoder to synchronize the library.

The mechanism behind the pattern matching and the template replenishing is briefly described as follows. Since the coefficient set template pattern library has only one standard coefficient set, no bit transmission is necessary. The residual coefficient set is thus obtained, which is the difference between the input coefficient set and the coefficient set in the library. If the residual is greater than the preset threshold, then the simple replenishing scheme is performed to update the coefficient set pattern library. The residual is then fed into a residual coding unit for further compression.

3.4 Residual Coding

Besides the codes for the standard coefficient set template patterns, an efficient coding method must be used to encode the residual coefficient set. In order to achieve higher compression ratio, a quantization process can be used to quantize the residual before encoding. In this section, a variable-length entropy coding method is introduced to encode the residual coefficient set.

The coding method employs a variable-length entropy coding (VLC) which is a combination of Huffman coding and run-length coding. In the transmitter, the variable-length encoder accepts data from the quantizer (Q). The quantization table

used in the quantizer is generated by using a simple uniform quantization which is specified by a quality factor, QF; that is,

$$Q[n] = QF, \qquad n = 1, 2, \ldots, T_s \tag{3.4.14}$$

where T_s is the number of coefficients in each coefficient set. Assume the unquantized residual coefficient sets $W_r = \{w_r(n), n = 1, 2, \ldots, T_s\}$, where $w_r(n)$ denotes the nth component of the unquantized data. Thus the nth component of the quantized residual is

$$x_q(n) = \frac{x_r(n)}{Q[n]}, \qquad n = 1, 2, \ldots, T_s. \tag{3.4.15}$$

The quantized data is first encoded with a run-length coding. It is converted into a sequence of runs between nonzero components and the magnitude of those nonzero components. Then, each event, consisting of a nonzero component and the corresponding run length of zeros, is further encoded with a specified Huffman code. In the receiver, the variable-length decoder accepts the bit stream from the transmission buffer and performs the inverse operations. Following the decoding process, the dequantization is performed to reconstruct the residual coefficient set.

3.5 Beat Reconstruction

The block schematic of the decoder is shown in Figure 3.5. The received encoded residual is first decoded by dequantization. Then the coefficients are reconstructed as the sum of the residual and the coefficient set template. Note that, the inverse DWT of these coefficients is computed to obtain the reconstructed normalized beats. The normalized beats are then multiplied by the corresponding amplitude scale

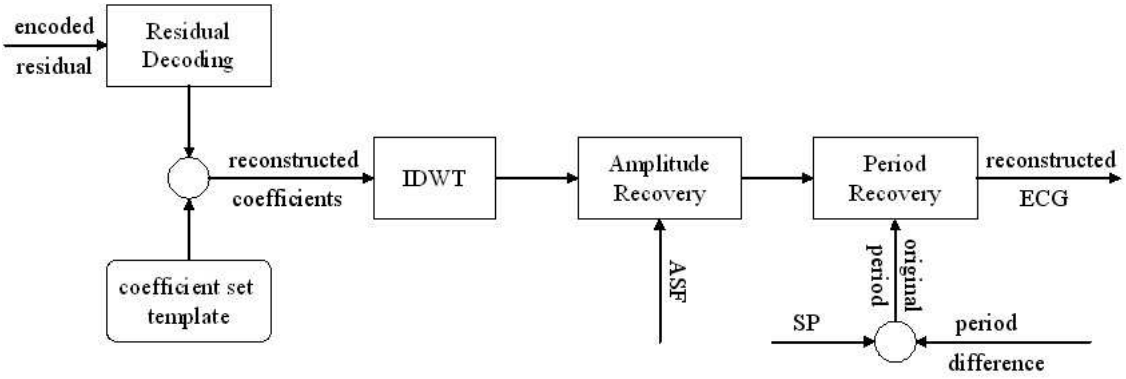

Figure 3.5: Block schematic of the decoder.

factors. The actual period of each beat is obtained from the period difference and the Standard Period. The original period beat is then recovered by multirate techniques as described in Section 3.4, from which follows the reconstructed ECG signal.

3.6 Experimental Results and Discussions

3.6.1 Experimental Results

The proposed method was tested on ECG data from MIT/BIH Arrhythmia Database [21], which was sampled at 360 Hz with 12 bit resolution. The performance of the method is evaluated using the measures discussed below. The compression (CR) has been computed as follows:

$$CR = \frac{K \sum_{i=1}^{N_T} T_i}{N_T(N_R b + \alpha_a + \alpha_p) + K N_M T_s + b_{sp} + b_h + b_t} \tag{3.6.16}$$

where K is the number of bits per sample in the original signal, T_i is the period of the ith beat, N_T is the total number of beats, N_R is the number of coefficients whose residuals are transmitted for each cycle, b, α_a, and α_p are the number of bits used for transmitting each residual, amplitude scale factor, and period difference,

Table 3.1: Compression ratio and PRD of three experimental records

Record	101	106	116
CR	22.7	28.5	24.6
PRD(%)	3.35	7.21	6.34

Table 3.2: Comparison of CR and PRD performance of our method (WBPM) with other techniques

Method	WBPM	Time series analysis	Linear prediction	WHOSC
CR	22.7–28.5	15.9	15–22	15.8-22.2
PRD(%)	3.35–7.21	4	9–13	1.73–1.75

respectively, b_{sp} is the number of bits used for transmitting standard period, N_M is the number of templates that have been used, T_s is the standard period, b_h and b_t are the number of bits for the samples preceding the first beat and those following the last beat.

The error measurement used here is the PRD as defined in Eq. (2.2.1). Figures 3.6 and 3.7 give the original, reconstructed, and the error waveforms, respectively, for two of the experimental signals. Table 3.1 gives the performance figures for three different experimental signals. It can be seen that the compression ratio (CR) achieved varies from 22.7 to 28.5. The method proposed is elegant and does not require a *priori* knowledge of the ECG waveform.

By observing the waveforms of the reconstructed signal, we can see that the morphology of all the components are well preserved . According to the results listed in Table 3.2, our method (WBPM) gains improvement on the coding performance in terms of CR versus PRD measure over some recent methods including time series

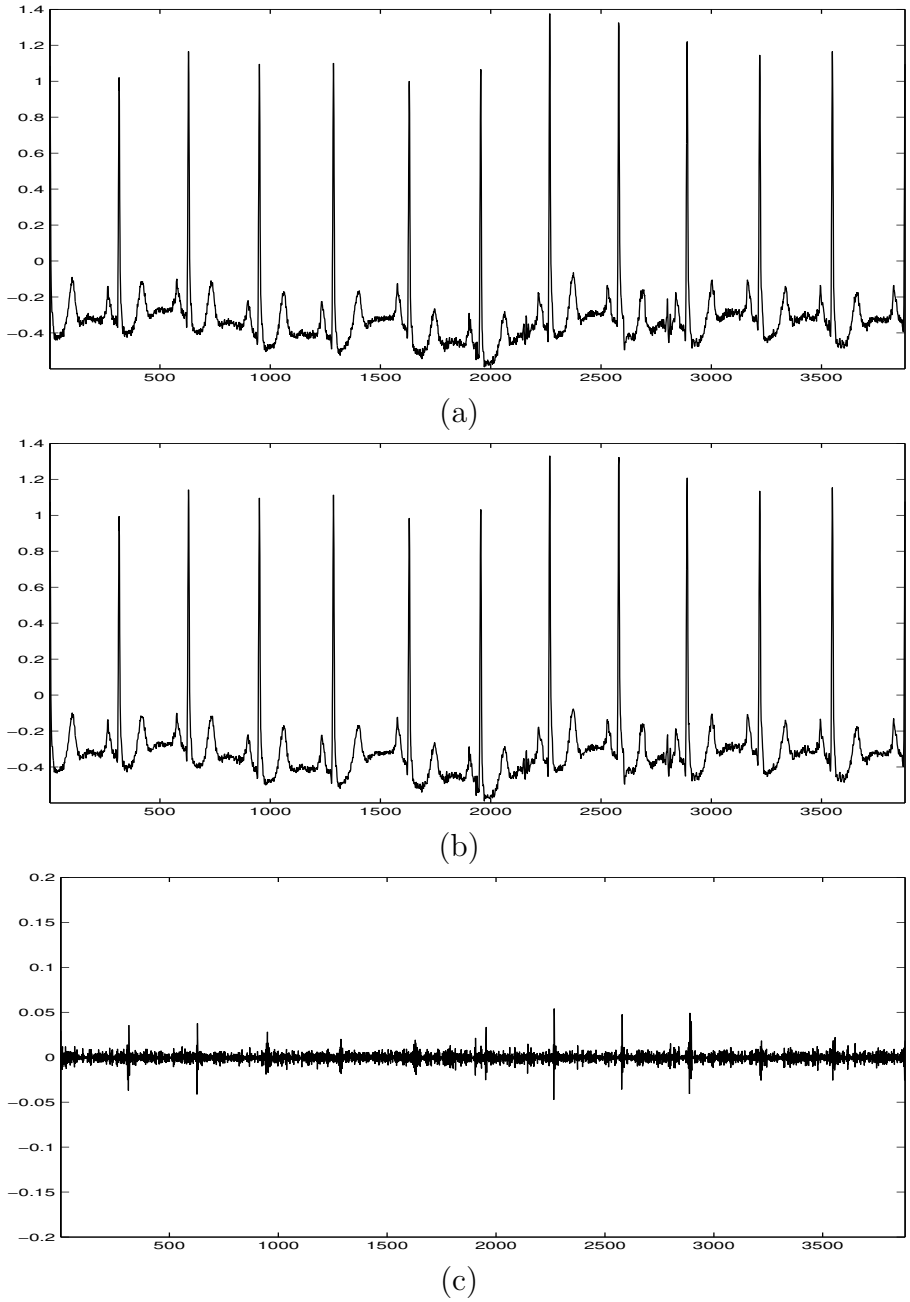

Figure 3.6: Results on record 101 from the MIT-BIH Arrythmia Database: (a) original ECG; (b) reconstructed signal; and (c) reconstruction error. The vertical axis represents the amplitude and the horizontal axis represents the sample index.

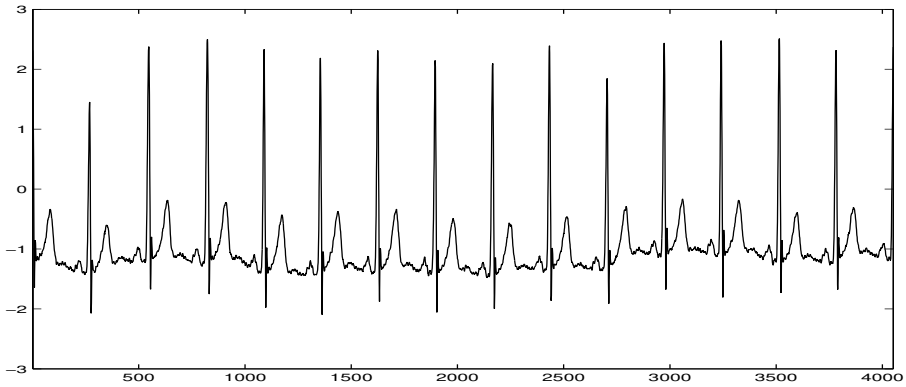

(a)

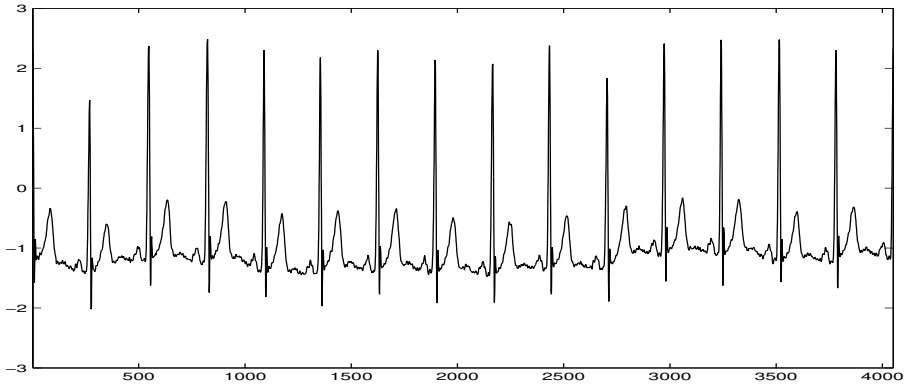

(b)

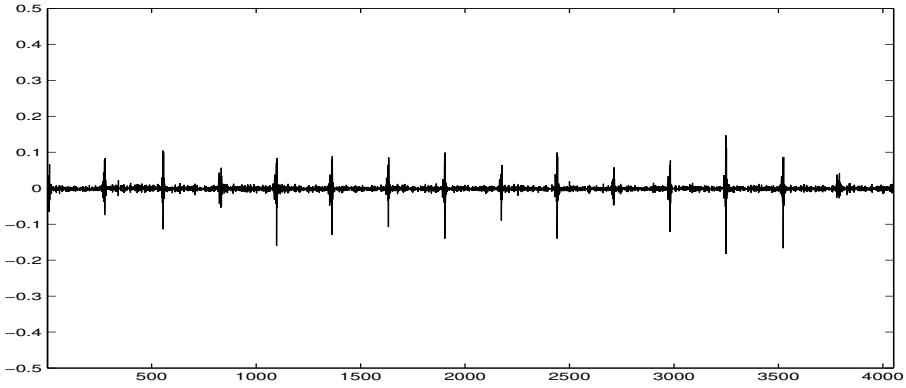

(c)

Figure 3.7: Results on record 116 from the MIT-BIH Arrythmia Database: (a) original ECG; (b) reconstructed signal; and (c) reconstruction error. The vertical axis represents the amplitude and the horizontal axis represents the sample index.

analysis [37], linear prediction [29] and WHOSC [38] for ECG data compression. We conclude that the achievement of the significant improvement on the coding performance is mainly due to the employment of the interbeat correlation, pattern matching and efficient residual coding in our method.

3.6.2 Discussions

Following beat delineation, the periods of the beats are normalized by multirate processing in order to minimize the effect of heart rate variability. Amplitude normalization is performed afterwards in order to bring further similarity between beats, and discrete wavelet transform is applied to each normalized beat. Due to the period and amplitude normalization, the wavelet transform coefficients bear a high correlation across beats. To increase the compression ratio, a pattern matching unit is utilized, and the residual sequence obtained is further encoded. The difference between the actual period and the standard period, and the amplitude scale factor are also retained for each beat and transmitted to the decoder. At the decoder, the inverse wavelet transform is computed from the reconstructed wavelet transform coefficients. The original amplitude and period of each beat are then recovered, which follows the original signal. This method has taken the advantage of correlation across and within beats of ECG signal for efficient compression. The simulation results show that our compression algorithm achieves a significant improvement in the performance of compression ratio and error measurement. Moreover, the morphological information is well preserved in the reconstructed signal, that is, the results are acceptable, which is of vital importance in telemedicine. The performance of the

algorithm can be improved by increasing the levels of pattern matching and utilizing more efficient residual coding, which is a recommendation for future work.

Chapter 4

Compression of ECG as a Signal with Finite Rate of Innovation

In this chapter, a new method of sampling and reconstruction of ECG data is proposed. The ECG signal is first modelled as the sum of bandlimited signal and nonuniform spline of degree one which contains a finite rate of innovation. A review of sampling signals with finite rate of innovation is given afterwards. Then the signal is sampled at the finite rate in order to achieve compression of the ECG signal. The original signal can be reconstructed given certain number of Fourier series coefficients. By comparing the simulation results with the ones achieved by classic sinc interpolation, it is shown that the performance of the proposed one is much better than the latter.

Figure 4.1 gives the block diagram of the processing procedures.

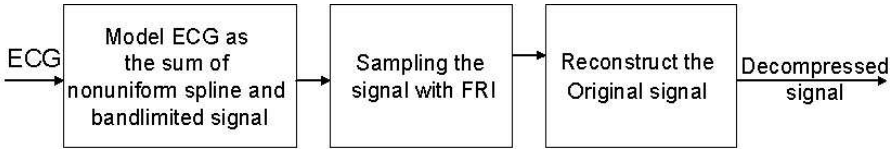

Figure 4.1: Block diagram of the algorithm.

4.1 Modelling of ECG as the Sum of Bandlimited and Nonuniform Spline of Degree One

From an engineering point of view, an ECG signal is quasi-periodic, and a P-QRS-T cycle consists one period of the signal. In order to preserve the diagnostic information in ECG signal, the QRS complex has to be well preserved in the modelled signal. From the analysis of the QRS complex, it is easy to see that it can be modelled as nonuniform linear spline. By subtracting the QRS complex from the original signal, the remaining part can be modelled as a bandlimited signal.

Firstly, for delineating cycles, we define a cycle as the signal from one R-peak to the next. We use the technique reported in [35] for QRS detection. Once we get the R-peaks of the ECG signal, a P-QRS-T cycle can be extracted from the original signal. From the analysis of the morphology of the QRS complex, it can be approximated as a nonuniform linear spline. From the transition points we get from the QRS detection, linear interpolation is performed to get the linear approximation. The number of pieces is determined by the number of transition points. By subtracting the QRS complex from the original signal, the remaining part of the signal is analyzed. It is shown that the remaining part can be modelled as a bandlimited signal. The bandwidth of the bandlimited approximation is determined by observing the distribution of the Fourier Spectrum. Thus, the sum of the nonuniform linear spline and bandlimited signal is an approximation of the original ECG signal. Figures 4.2, 4.3 and 4.4 show examples of approximating ECG signal as bandlimited plus nonuniform linear spline. We can easily see that the shape of the

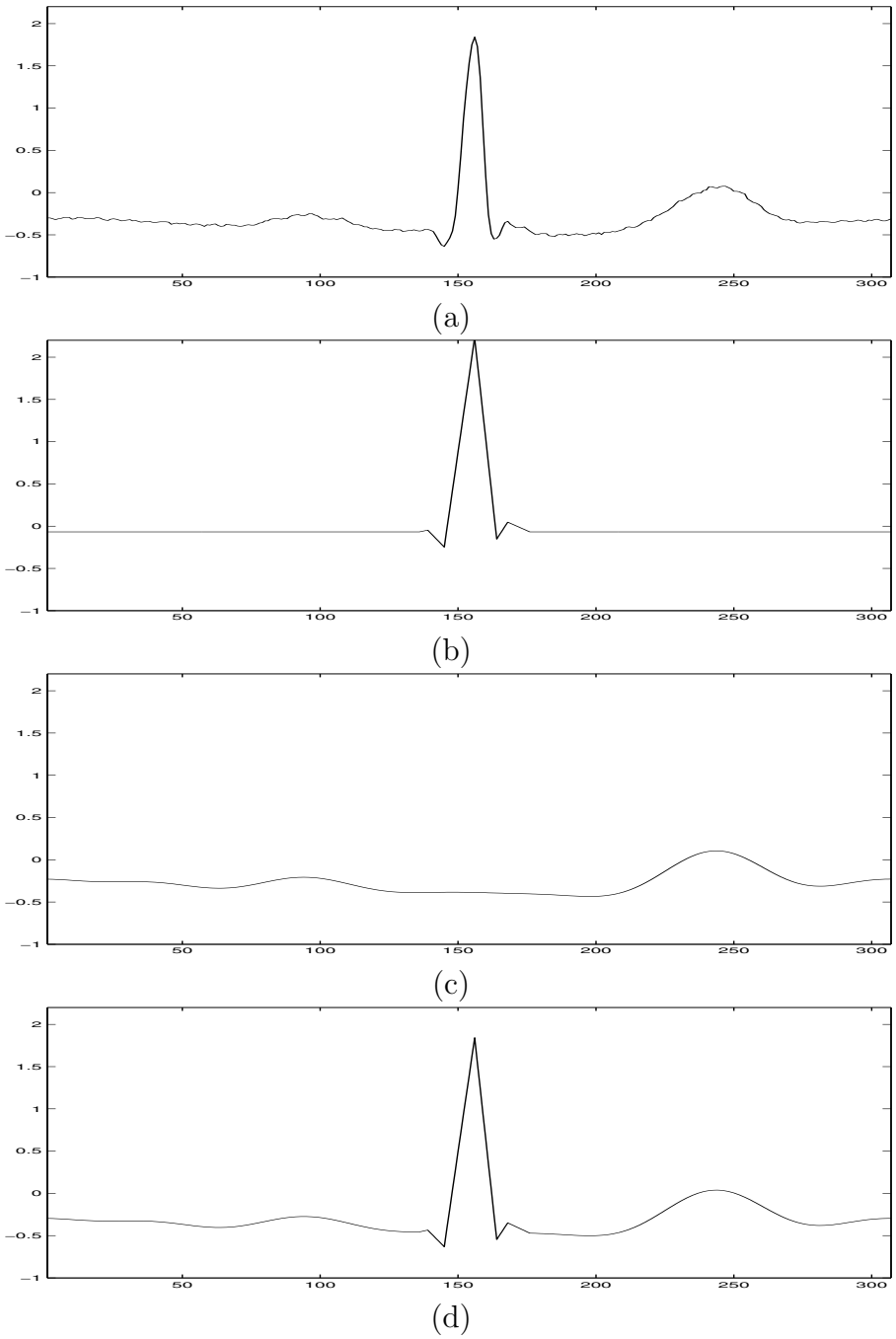

Figure 4.2: Modelling of ECG103 as bandlimited plus nonuniform linear spline. (a) the original ECG signal; (b) the nonuniform spline approximation of the peak; (c) the bandlimited approximation of the remaining part of the signal; (d) the sum of the nonuniform linear spline and bandlimited signal. The vertical axis represents the amplitude and the horizontal axis represents the sample index.

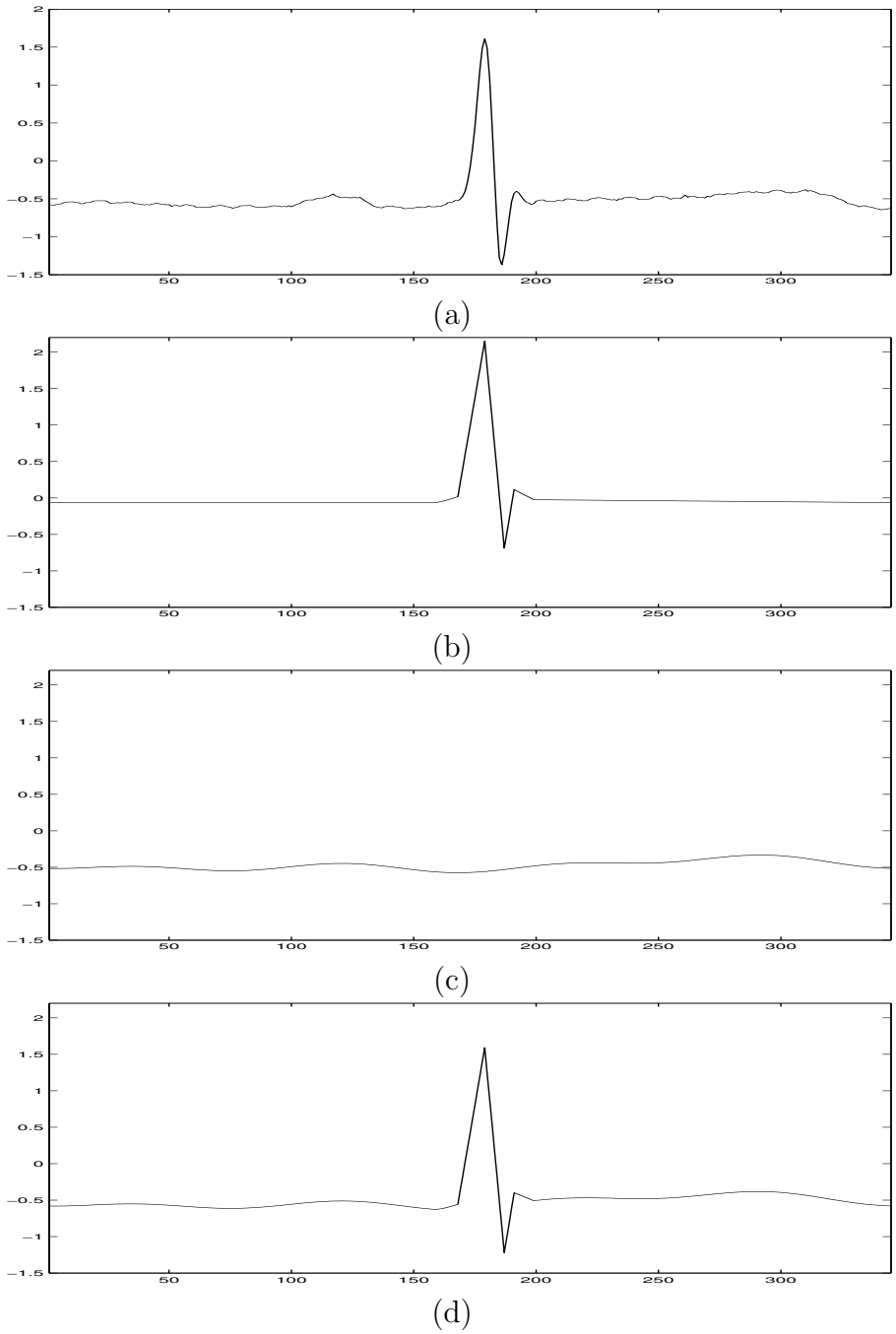

Figure 4.3: Modelling of ECG115 as bandlimited plus nonuniform linear spline. (a) the original ECG signal; (b) the nonuniform spline approximation of the peak; (c) the bandlimited approximation of the remaining part of the signal; (d) the sum of the nonuniform linear spline and bandlimited signal. The vertical axis represents the amplitude and the horizontal axis represents the sample index.

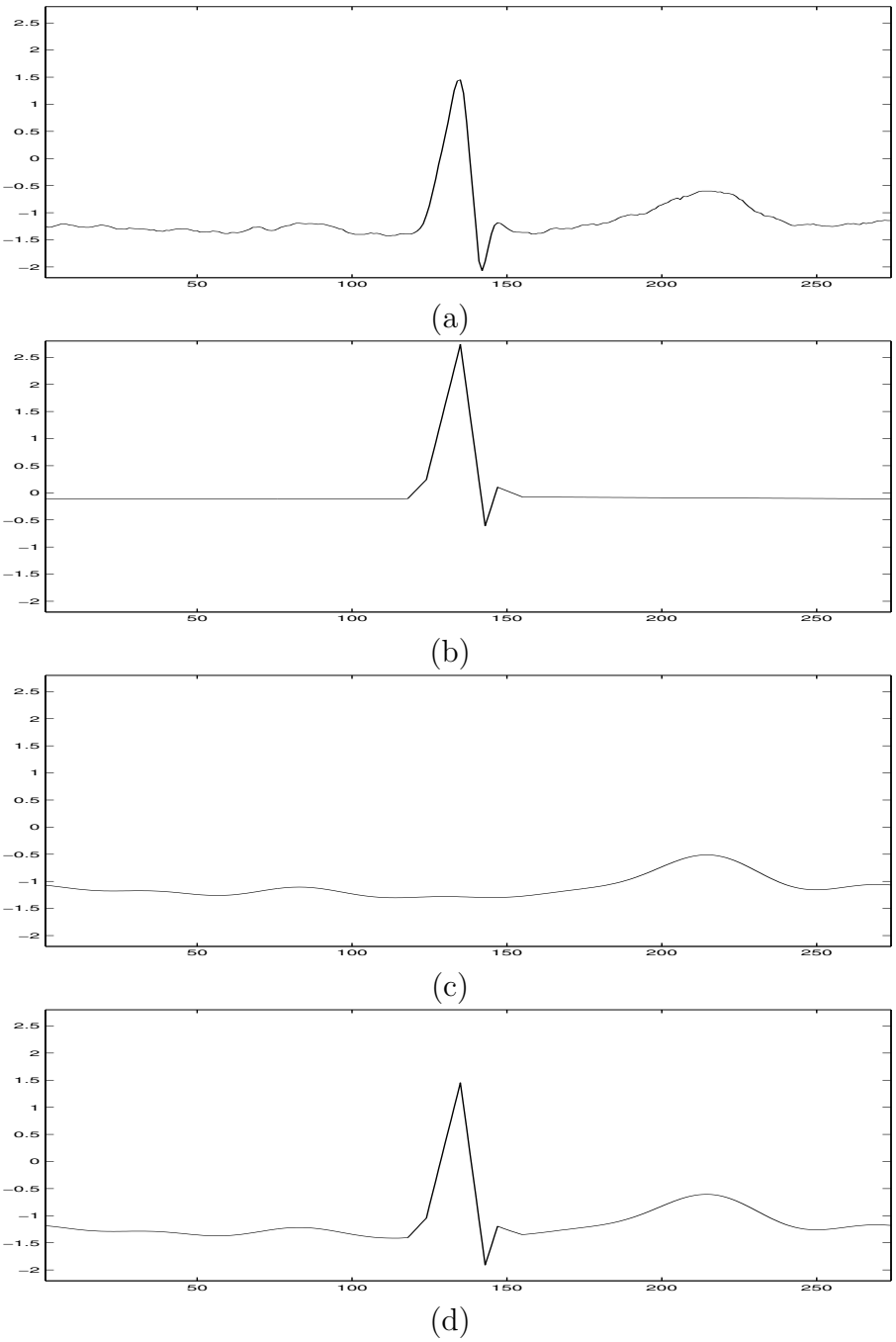

Figure 4.4: Modelling of ECG116 as bandlimited plus nonuniform linear spline. (a) the original ECG signal; (b) the nonuniform spline approximation of the peak; (c) the bandlimited approximation of the remaining part of the signal; (d) the sum of the nonuniform linear spline and bandlimited signal. The vertical axis represents the amplitude and the horizontal axis represents the sample index.

original signal is well preserved in the approximated one.

4.2 Review on Sampling Signals with Finite Rate of Innovation

Consider classes of signals which have a finite number of degrees of freedom per unit of time, and call this number the rate of innovation. Examples of signals with a finite rate of innovation include streams of Dirac pulses, non-uniform splines and piecewise polynomials.

Even though these signals are not bandlimited, it has been shown that they can be sampled uniformly at (or above) the rate of innovation using an appropriate kernel, and then be perfectly reconstructed. Sampling theorems have been proved for classes of signals and kernels that generalize the classic "bandlimited and sinc kernel" case in [39–43]. The key in all constructions is to identify the innovative part of a signal (e.g. time instants and weights of Diracs) using an annihilating or locator filter, a device well known in spectral analysis and error correction coding [39].

In particular, we will give a review on how to sample and reconstruct periodic streams of Dirac pulses and nonuniform splines in the following subsections.

4.2.1 Signals with Finite Rate of Innovation

The classic sampling theorem relies on the fact that the signal is bandlimited, but what if the signal is not bandlimited? How can the signal be sampled and reconstructed? One way is to make it bandlimited, in other words, take a lowpass

approximation of the signal and then apply the classic sampling and reconstruction scheme, but the result is far from satisfactory [41].

For bandlimited signals, they are completely determined by sampling the signal at a rate of 1 sample every T seconds, that is, the signal has $1/T$ degrees of freedom per unit of time. So it is interesting to see if we can sample and reconstruct non-bandlimited signals that are characterized as having finite degrees of freedom per unit of time. These signals are defined as signals with a finite rate of innovation. Formally, the rate of innovation ρ is the average number of degrees of freedom per unit of time, or, with $C_x(t_a, t_b)$ giving the number of degrees of freedom of $x(t)$ over the interval $[a, b]$,

$$\rho = \lim_{\tau \to \infty} \frac{1}{\tau} C_x\Big(-\frac{\tau}{2}, \frac{\tau}{2}\Big) \tag{4.2.1}$$

Examples are stream of Diracs, nonuniform splines and piecewise polynomials.

In the following subsections, we consider $\tau-$periodic stream of Diracs and nonuniform splines. The natural representation of such periodic signals is given by Fourier series

$$x(t) = \sum_{m \in \mathbb{Z}} X[m]\, e^{i\frac{2\pi m t}{\tau}}. \tag{4.2.2}$$

Such signals can be recovered uniquely from a certain number of contiguous Fourier coefficients, and these coefficients can be obtained from the samples of the original signals.

4.2.2 Periodic Stream of Diracs

Consider a stream of K Diracs periodized with period τ, $x(t) = \sum_{n\in\mathbb{Z}} c_n\,\delta(t-t_n)$ where $t_{n+K} = t_n + \tau$ and $c_{n+K} = c_n, \forall n \in \mathbb{Z}$. This signal has $2K$ degrees of freedom per period (K from the locations and K from the weights), thus the rate of innovation is

$$\rho = \frac{2K}{\tau}. \tag{4.2.3}$$

The periodic stream of Diracs can be rewritten as

$$\begin{aligned} x(t) &= \sum_{k=0}^{K-1} c_k \sum_{n\in\mathbb{Z}} \delta(t - t_k - n\tau) \\ &= \sum_{k=0}^{K-1} c_k \frac{1}{\tau} \sum_{m\in\mathbb{Z}} e^{i\frac{2\pi m(t-t_k)}{\tau}} \qquad \text{from Poisson's summation formula} \\ &= \sum_{m\in\mathbb{Z}} \underbrace{\frac{1}{\tau}\Big(\sum_{k=0}^{K-1} c_k\, e^{-i\frac{2\pi m t_k}{\tau}}\Big)}_{X[m]}\, e^{i\frac{2\pi m t}{\tau}}. \end{aligned} \tag{4.2.4}$$

The Fourier series coefficients $X[m]$ are thus given by

$$X[m] = \frac{1}{\tau}\sum_{k=0}^{K-1} c_k\, e^{-i\frac{2\pi m t_k}{\tau}}, \quad m \in \mathbb{Z} \tag{4.2.5}$$

that is, the linear combination of K complex exponentials.

Theorem 4.1. *[39] Consider $x(t)$, a periodic stream of Diracs of period τ with K Diracs of weight $\{c_k\}_{k=0}^{K-1}$ and at location $\{t_k\}_{k=0}^{K-1}$ as in Eq. (4.2.4). Take as sampling kernel $h_B(t) = B\,sinc(Bt)$ where B is chosen such that it is greater or equal to the rate of innovation ρ given by (4.2.3), and sample $(h_B * x)(t)$ at N uniform locations $t = nT, n = 0, \ldots, N-1$, where $N \geq 2M+1$ and $M = \lfloor \frac{B\tau}{2} \rfloor$. Then the samples*

$$y_n =< h_B(t - nT), x(t) >, \quad n = 0, \ldots, N-1 \tag{4.2.6}$$

are a sufficient characterization of $x(t)$.

Algorithm 4.1. *The algorithm of sampling and reconstruction of stream of Diracs is described as follows:*

1. *Calculate the sample values.*

   $y_n =< h_B(t - nT), x(t) >, \quad n = 0, \ldots, N-1$, *we take* T *as a divisor of* τ *here, then* $N = \tau/T$. *Let* $B = \rho$, *we have* $M = K$.

2. *Finding* $X[m], |m| \leq K$ *from* $y_n, n = 0, \ldots, N-1$.

   Using Eq. (4.2.2) in (4.2.6) we have

$$y_n = \sum_m X[m] \; < h_B(t - nT), e^{i\frac{2\pi mt}{\tau}} > \tag{4.2.7}$$

$$= \sum_m X[m] \, H_B(\frac{2\pi m}{\tau}) \, e^{i\frac{2\pi mnT}{\tau}} \tag{4.2.8}$$

$$= \sum_{m=-K}^{K} X[m] \, e^{i\frac{2\pi mnT}{\tau}} \tag{4.2.9}$$

   where $H_B(\omega) = Rect(\frac{\omega}{2\pi B})$ *is the Fourier transform of* $h_B(t)$. *The* $2K+1$ *contiguous coefficients can be obtained by solving this system of equations. Note that* $N = \tau/T$, y_n *corresponds to the IDFT of* $X[m]$.

3. *Finding the coefficients of the filter* $A[m]$ *that annihilates* $X[m], m \in [-K, K]$.

   Given $X[m], m = -K, \ldots, K$, *solve Eq. (4.2.10) for* $A[m], m = 1, \ldots, K$,

$$A[m] * X[m] = 0. \tag{4.2.10}$$

   This is a classic Yule-Walker system [44], which in our case has a unique solution when there are K *distinct Diracs in* $x(t)$ *because there is a unique annihilating filter.*

4. *Finding K locations.*

   Given the coefficients $1, A[1], \ldots, A[K]$, we factor its $z-$ transform into its roots

$$A(z) = \prod_{k=0}^{K-1} (1 - u_k\, z^{-1}) \tag{4.2.11}$$

   where $u_k = e^{-i\frac{2\pi t_k}{\tau}}$, which leads to the K locations $\{t_k\}_{k=0}^{K-1}$.

5. *Finding the weights c_k.*

   Given the locations $\{t_k\}_{k=0}^{K-1}$, we can write K values of $X[k]$ as linear combinations of exponentials. In general, using $u_k = e^{-i\frac{2\pi t_k}{\tau}}$, since t_k's are distinct, we have a Vandermonde system, which will always lead to a solution of c_k's.

4.2.3 Periodic Nonuniform Splines

In this section we consider periodic nonuniform splines of period τ. A signal $x(t)$ is a periodic nonuniform spline of degree R with knots at $\{t_k\}_{k=0}^{K-1} \in [0, \tau]$ if and only if its $(R+1)$th derivative is a periodic stream of K weighted Diracs $x^{(R+1)}(t) = \sum_{n\in\mathbb{Z}} c_n\, \delta(t - t_n)$ where $t_{n+K} = t_n + \tau$ and $c_{n+K} = c_n, \forall n \in \mathbb{Z}$. Thus the rate of innovation is

$$\rho = \frac{2K}{\tau}. \tag{4.2.12}$$

Using Eq. (4.2.4) we can state that the Fourier series coefficients of $x^{(R+1)}(t)$ are $X^{(R+1)}[m] = \frac{1}{\tau} \sum_{k=0}^{K-1} c_k\, e^{-i2\pi m t_k}$. Differentiating Eq. (4.2.2) $R+1$ times shows that these coefficients are

$$X^{(R+1)}[m] = (i2\pi m/\tau)^{R+1}\, X[m], \quad m \in \mathbb{Z}. \tag{4.2.13}$$

Theorem 4.2. *[39] Consider a periodic nonuniform spline $x(t)$ with period τ, containing K pieces of maximum degree R. Take a sinc sampling kernel $h_B(t)$ such that B is greater or equal to the rate of innovation ρ given by (4.2.12), and sample $(h_B * x)(t)$ at N uniform locations $t = nT, n = 0, \ldots, N-1$, where $N \geq 2M+1$ and $M = \lfloor \frac{B\tau}{2} \rfloor$. Then $x(t)$ is uniquely represented by the samples*

$$y_n =< h_B(t - nT), x(t) >, \quad n = 0, \ldots, N-1. \tag{4.2.14}$$

Algorithm 4.2. *The algorithm of sampling and reconstruction of periodic nonuniform splines is described as follows:*

1. *Calculate the sample values.*

   $y_n =< h_B(t - nT), x(t) >, \quad n = 0, \ldots, N-1$, *we take T as a divisor of τ here, then $N = \tau/T$. Let $B = \rho$, we have $M = K$.*

2. *Find $X[m]$, for $m \in [-K, K]$, that is $2K$ contiguous spectral values of $x(t)$ from the sample values. See Step 2 in Algorithm 4.1.*

3. *Find $2K$ contiguous spectral values of the stream of Diracs.*

   $X^{(R+1)}[m] = (i2\pi m/\tau)^{R+1} X[m], \quad m \in [-K, K]$. *See Steps 3 and 4 in Algorithm 4.1.*

4. *Determine the locations and weights of the Diracs $x^{(R+1)}(t)$ using annihilating filter method.*

5. *Get the original splines by integrating $R+1$ times the stream of Dirac pulse.*

The block diagram of the process is shown in Figure 4.5.

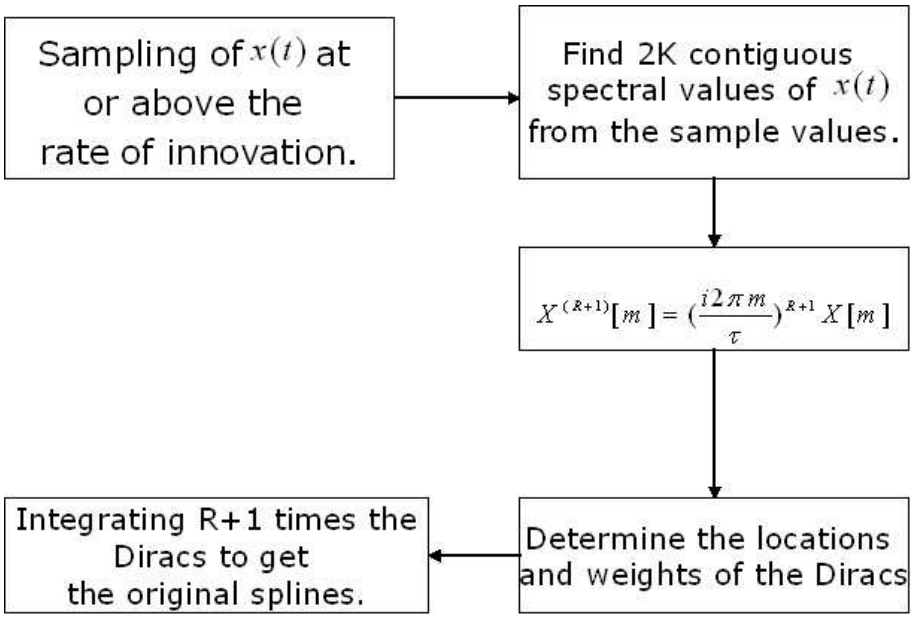

Figure 4.5: The block diagram of sampling procedures of nonuniform splines.

4.3 Compression and Reconstruction of ECG Signal

In this stage, the sampling theorem for signals with finite rate of innovation will be applied to compress and reconstruct the ECG signal. According to the method in Section 4.2, given the number of pieces in nonuniform linear spline and the bandwidth of the bandlimited signal, the sum of these two signals can be perfectly reconstructed.

We approximate the QRS complex as a nonuniform linear spline with K pieces, and the rest of the signal is approximated as a bandlimited signal with bandwidth of L, where the period of the original signal is τ. Then the modelled signal x is defined by

$$x(t) = x_{BL}(t) + x_{NS}(t), \tag{4.3.15}$$

with corresponding CTFS coefficients defined by

$$X[m] = \begin{cases} X_{BL}[m] + X_{NS}[m] & \text{if } m \in [-L, L] \\ X_{NS}[m] & \text{if } m \notin [-L, L]. \end{cases}$$

Consider the nonuniform spline of degree one with K pieces, it can be recovered from $2K$ contiguous frequency values $X_{NS}[m]$. Therefore it is sufficient to take $2K$ CTFS coefficients outside of the band $[-L, L]$, for instance in $[L+1, L+2K]$. From these $2K$ contiguous values, we can get the reconstruction of the nonuniform spline. Then the CTFS of the bandlimited signal are obtained by subtracting $X_{NS}[m]$ from $X[m]$ for $m \in [-L, L]$. It follows that we can sample the signal using a sinc kernel bandlimited to $2K + L$. The sum of the bandlimited signal and nonuniform linear spline can be reconstructed perfectly.

Algorithm 4.3. *The algorithm of sampling and reconstruction of ECG signal is described as follows:*

1. *Calculate the sample values.*

   $y_n =< h_B(t - nT), x(t) >, \quad n = 0, \ldots, N-1$, *we take* T *as a divisor of* τ *here, then* $N = \tau/T$. *Let* $B = \rho = (2K + L)/\tau$, *where* τ *is the period of the signal.*

2. *Find* $2K + L$ *contiguous spectral values of* $x(t)$ *from the sample values.*

3. *Find* $2K$ *contiguous values of* $X_{NS}[m]$ *by taking* $2K$ *CTFS coefficients of* $X[m]$ *outside the band of* $[-L, L]$, *for instance in* $[L + 1, L + 2K]$. *See step 2 in Algorithm 4.1.*

4. *Find $2K$ contiguous spectral values of the stream of Diracs.*

   $X_{NS}^{(R+1)}[m] = (i2\pi m/\tau)^{R+1} X_{NS}[m], \quad m \in [L+1, L+2K].$

5. *Determine the locations and weights of the Diracs $x^{(R+1)}(t)$ using annihilating filter method. See steps 3 and 4 in Algorithm 4.1.*

6. *Get the original spline $x_{NS}(t)$ by integrating $R+1$ times the Diracs, thus we have $X_{NS}[m]$, $m \in \mathbb{Z}$.*

7. *Find the bandlimited signal $x_{BL}(t)$. Once we get $X_{NS}[m]$, we have $X_{BL}[m] = X[m] - X_{NS}[m]$, where $m \in [-L, L]$, $x_{BL}(t)$ is thus recovered.*

8. *The original signal is the sum of the bandlimited signal and nonuniform linear spline.*

The block diagram of the process is shown in Figure 4.6.

4.4 Experimental Results and Discussions

4.4.1 Experimental Results

The proposed method was tested on ECG data from MIT/BIH Arrhythmia Database [21]. Figures 4.7, 4.8 and 4.9 give the original, reconstructed signal using sampling signal with FRI and sinc kernel, respectively. It is shown that sampling the ECG signal at its finite rate of innovation performs better in preserving the morphological and diagnostic information in ECG signal. Table 4.1 gives the reconstruction performance measurements for four different experimental signals. We get smaller reconstruction error by comparing our method with the classic sampling using sinc

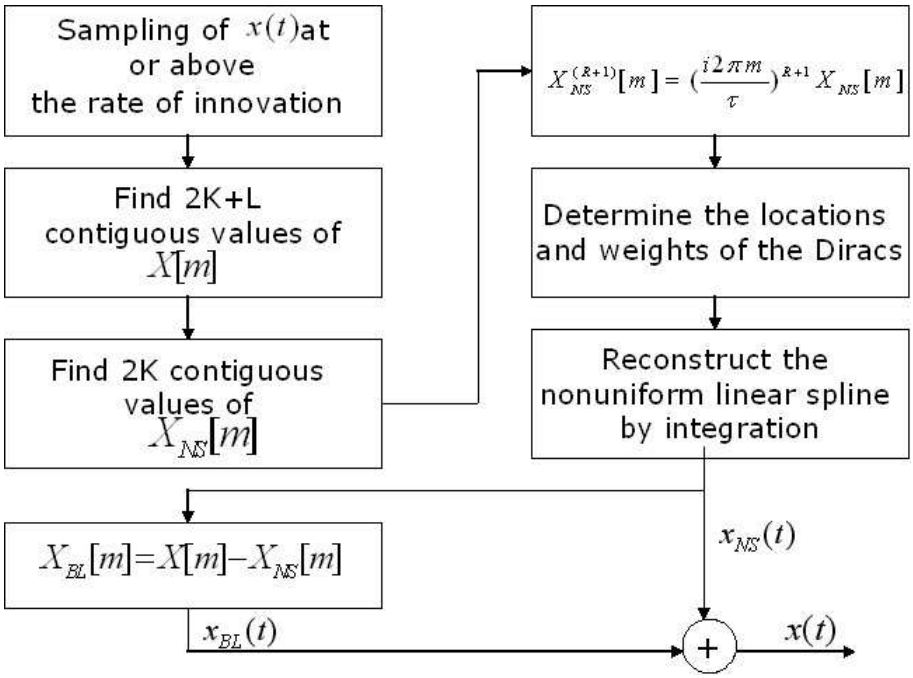

Figure 4.6: The block diagram of sampling procedures of bandlimited signal plus nonuniform splines.

interpolation. In both methods, $2K + L$ spectral values are used for reconstruction, the Compression Ratio (CR) is defined as the ratio of the number of samples in the original ECG signal and $2K + L$, the comparison is based on the same compression ratio. Table 4.2 gives the compression ratio for some of the signals from the database, the ratios are quite satisfactory.

Table 4.1: Comparison of reconstruction error of sampling with FRI and sinc kernel

Record	103	115	116	123
FRI	8.4%	7.7%	3.4%	2.8%
sinc	11.7%	12.7%	3.5%	5.9%

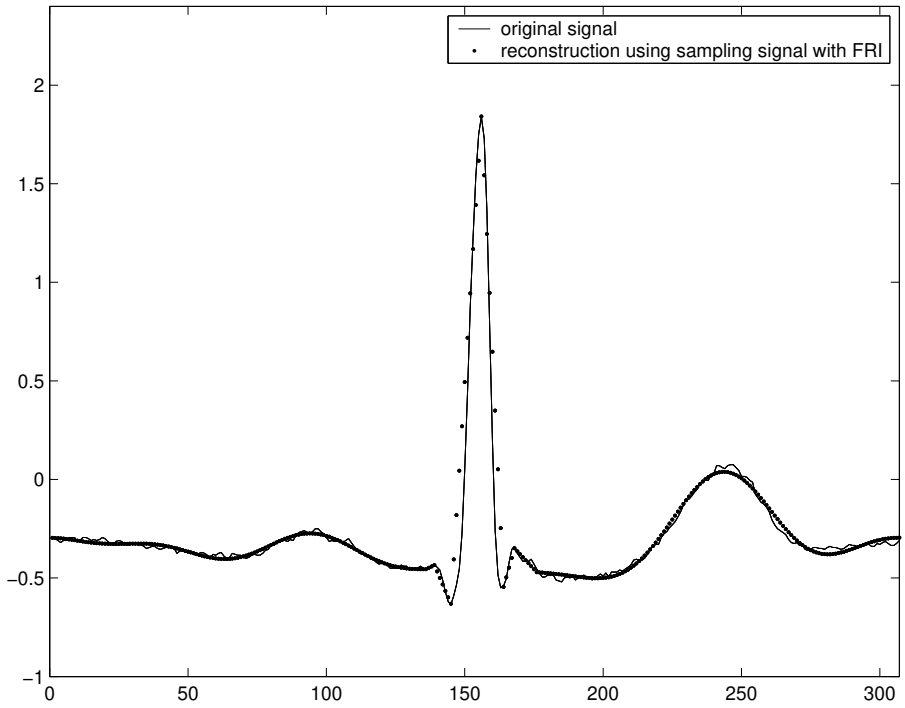

(a)

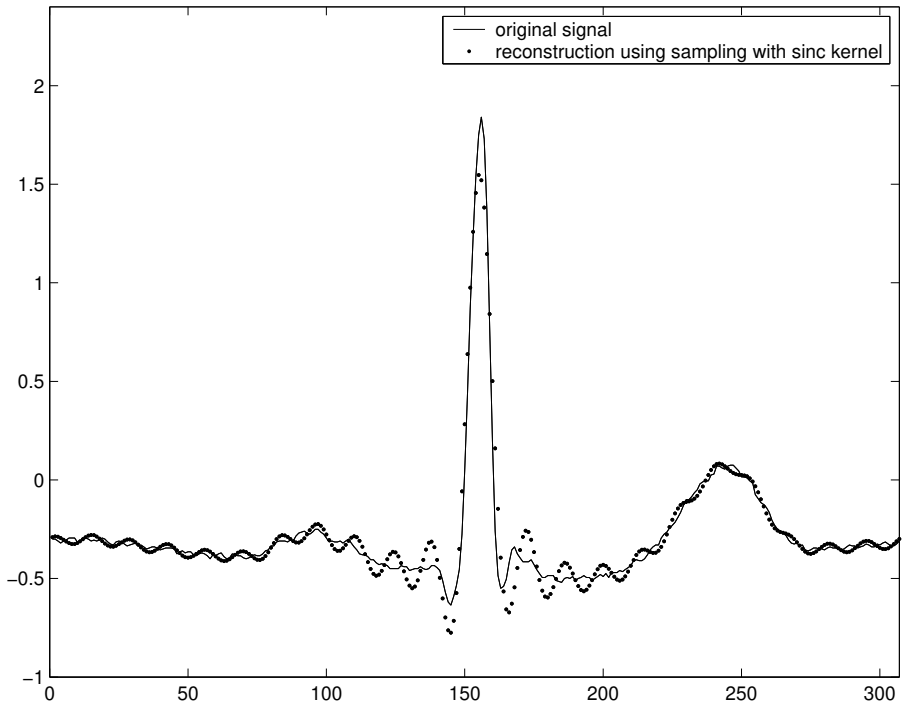

(b)

Figure 4.7: Results on record 103 from the MIT-BIH Arrythmia Database: (a) reconstruction of ECG using sampling signal with finite rate of innovation, with reconstruction error of 19%; (b) reconstruction of ECG using sampling with sinc kernel, with reconstruction error of 17%. The vertical axis represents the amplitude and the horizontal axis represents the sample index.

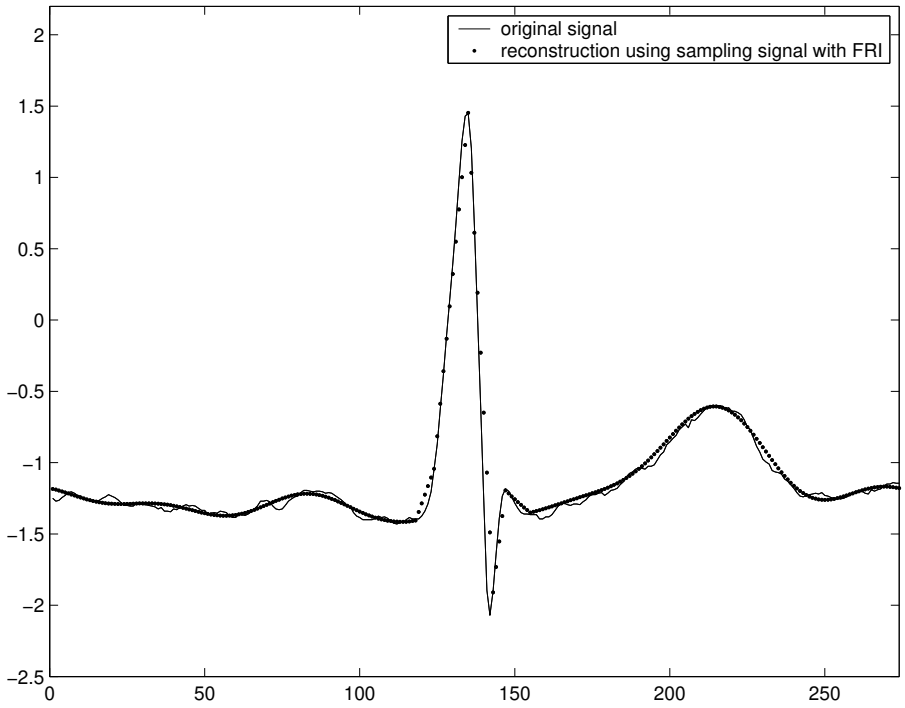

(a)

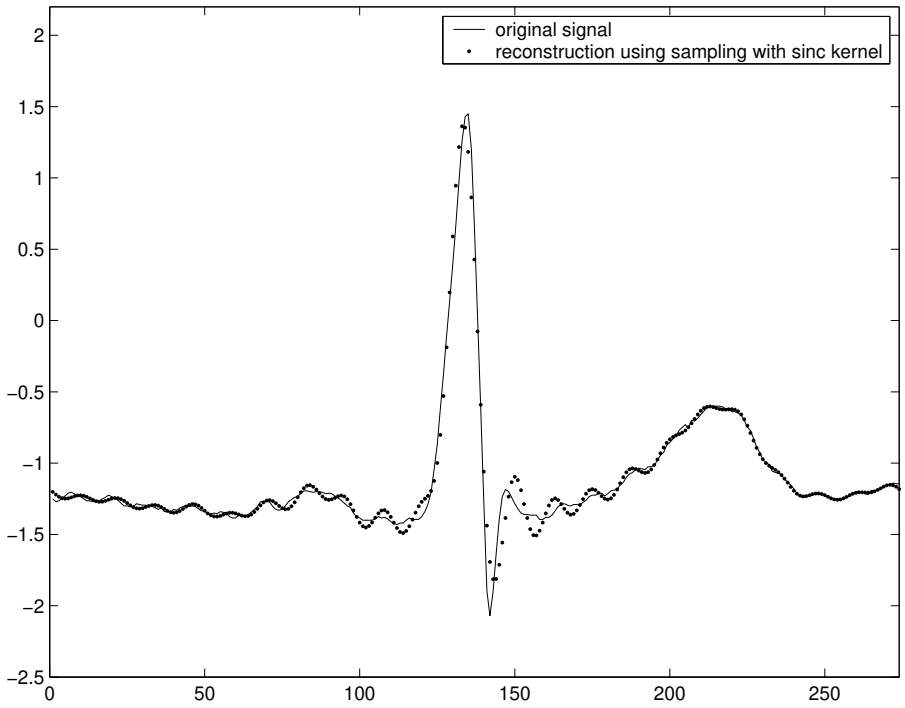

(b)

Figure 4.8: Results on record 116 from the MIT-BIH Arrythmia Database: (a) reconstruction of ECG using sampling signal with finite rate of innovation, with reconstruction error of 7%; (b) reconstruction of ECG using sampling with sinc kernel, with reconstruction error of 6%. The vertical axis represents the amplitude and the horizontal axis represents the sample index.

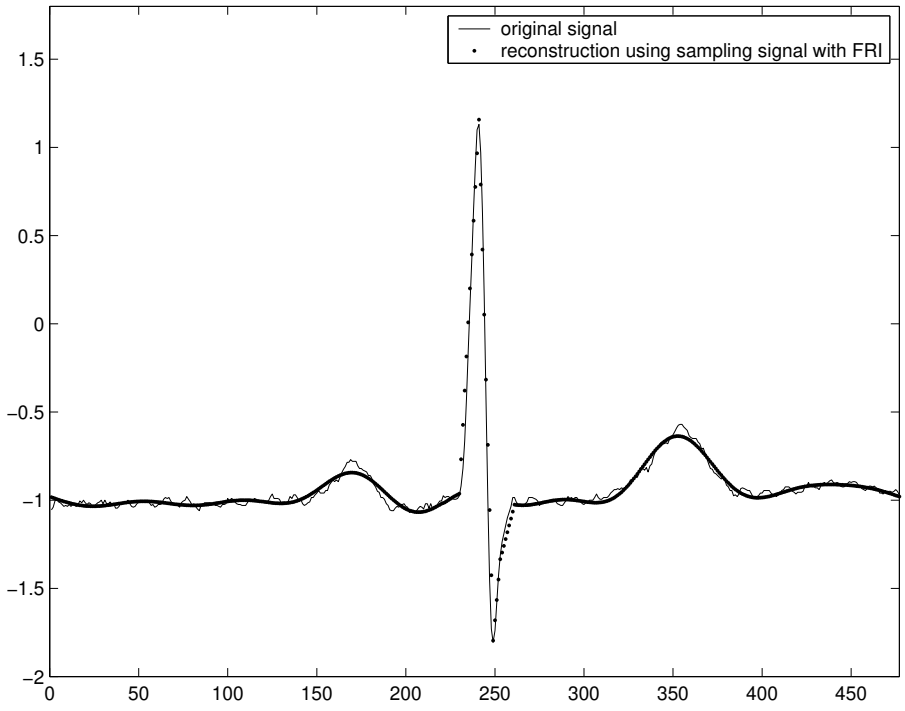

(a)

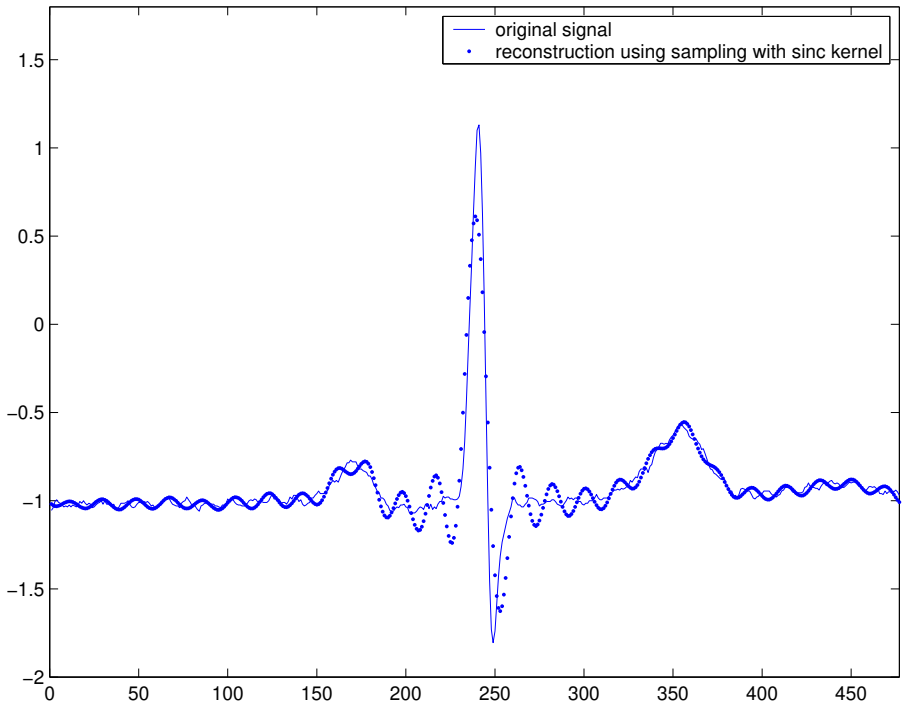

(b)

Figure 4.9: Results on record 123 from the MIT-BIH Arrythmia Database: (a) reconstruction of ECG using sampling signal with finite rate of innovation, with reconstruction error of 5%; (b) reconstruction of ECG using sampling with sinc kernel, with reconstruction error of 11%. The vertical axis represents the amplitude and the horizontal axis represents the sample index.

Table 4.2: Compression ratio performance on signals form MIT-BIH Arrythmia Database

Record	103	115	116	123
K	8	8	8	8
L	6	4	4	9
CR	14.0	17.3	12.5	19.1

4.4.2 Discussions

A novel algorithm for ECG data sampling and reconstruction has been proposed in this chapter. Firstly, we model ECG signal as the sum of bandlimited signal and nonuniform spline of degree one. Given the $2K+L$ coefficients of $X[m]$, the nonuniform spline is recovered from $2K$ of contiguous Fourier series coefficients outside the band of $m \in [-L, L]$. Once we get the nonuniform spline from these contiguous coefficients, the Fourier series coefficients of the bandlimited signal, X_{BL}, is obtained by subtracting X_{NS} from $X[m]$ inside the band of $m \in [-L, L]$. Generally speaking, the original signal can be reconstructed given certain number of Fourier series coefficients. By comparing the simulation results with the ones achieved by classic sinc interpolation, it is shown that the performance of the proposed one is much better than the latter, especially in preserving the morphological information of the signal, which is an important factor in biomedical signal processing. The performance of this algorithm can be improved by decreasing K and L in modelling of ECG signal. Finding an optimal method of modelling ECG signal with minimum parameters K and L is a recommendation for future work.

Chapter 5

Conclusions and Recommendations for Future Research

5.1 Conclusions

The objective of our study is to develop effective compression schemes for ECG data transmission and storage. Review on data compression and conventional methods for ECG compression are given in the first part of this thesis and two methods for high fidelity coding of ECG have been proposed.

Handling R-R beats eliminates the ambiguity that normally arises in deciding the endpoints of a cycle whenever PQRST beats are used. The normalization preprocessing converts the ECG data into a near-cyclostationary sequence. A Wavelet transform is then performed on the normalized beats and the wavelet coefficients of consecutive beats show high correlation. Accordingly, we focus our attention on the design of a pattern matching unit for efficient compression. An efficient residual coding is then performed to achieve further compression. The wavelet-based pat-

tern matching method performs well with normal data and achieves a significantly high CR performance with low distortion. As compared with other methods, our technique is very efficient. The advantage of this technique is that it can be applied to other semi-periodic biomedical signals. Moreover, this technique can be utilized for off-line applications such as patient databases and medical education systems.

As for the method of compressing ECG as signals with finite rate of innovation, we have taken the advantage of morphology of ECG signal, which can be modelled as a bandlimited signal plus nonuniform spline of degree one. By applying the sampling methods for signals with finite rate of innovation, ECG signal is sampled at its finite rate of innovation and the original signal can be reconstructed given certain number of Fourier series coefficients. Thus, compression of ECG is achieved. Judging from the experimental results, diagnostic information is well preserved in the reconstructed signals.

5.2 Recommendations for Future Research

The potential topics in the future are described as follows:

A one-stage pattern matching is performed in the first method. In order to obtain a residual coefficient set with an even smaller variance, a two-stage pattern matching unit can be utilized. For residual coding process, other methods, such as vector quantization, should be implemented in order to achieve possibly more efficient coding.

Since PRD is only an average measure, it alone cannot adequately quantify the

diagnostic acceptability of the reconstructed signal. The QRS complex of the ECG carries significant morphological information, and the error in this region must not be excessive. New distortion measures which can show the diagnostic acceptability of the reconstructed signal should be developed in the future.

The methods proposed are designed just for single-channel ECG, while in practical application, multi-channel ECG is widely used. Methods for single-channel data compression will be generalized for efficient compression of multi-channel ECG data.

Optimal modelling of the ECG as a signal with finite rate of innovation can be investigated to yield more efficient compression and accurate reconstruction.

Moreover, regarding the proposed method of compressing ECG as a signal with finite rate of innovation, if relocation of functionalities can be done between encoder and decoder, for instance, reconstruction of the non-uniform spline is done in the encoder, only segment end points need to be transmitted along with the spectral values used for reconstruction of bandlimited signal, higher compression might be achieved while achieving similar performance of the proposed one. This can be a potential method for further investigation.

Since many biomedical signals are periodic in an engineering point of view, which is similar to ECG, general algorithms will be developed for these kind of signals. Since these signals convey significant information of the human body, such algorithms will contribute to the advancement of telemedicine.

Author's Publications

1. "An Efficient Wavelet-based Pattern Matching Scheme for ECG Data Compression", Yanyan Hao and Pina Marziliano, IEEE International Workshop on Biomedical Circuits & Systems, Singapore, 1-3 December 2004.

2. "Compression of ECG as Signal with Finite Rate of Innovation", Yanyan Hao, Pina Marziliano, Martin Vetterli and Thierry Blu, 27th Annual International Conference of the IEEE Engineering in Medicine and Biological Society (EMBS), Shanghai, China, September 1-4, 2005.

Bibliography

[1] P. W. Hsia, "Electrocardiographic data compression using precoding consecutive QRS information," *IEEE Trans. Biomed. Eng.*, vol. 36, pp. 465–468, 1989.

[2] P. S. Hamilton and W. J. Tompkins, "Compression of the ambulatory ECG by average beat subtraction and residual differencing," *IEEE Trans. Biomed. Eng.*, vol. 38, pp. 253–259, 1991.

[3] W. B. Kleijn and K. K. Paliwal, *Speech Coding and Synthesis.* Amsterdam: Elsevier, 1995.

[4] G. Nave and A. Cohen, "ECG compression using long-term prediction," *IEEE Trans. Biomed. Eng.*, vol. 40, pp. 877–885, Sept. 1993.

[5] D. J. Hamilton, D. C. Thomson, and W. A. Sandham, "ANN compression of morphologically similar ECG complexes," *Med. and Biol. Eng. and Comp.*, vol. 33, pp. 841–843, 1995.

[6] J. P. Abenstein and W. J. Tompkins, "A new data reduction algorithm for real time ECG analysis," *IEEE Trans. Biomed. Eng.*, vol. BME-29, pp. 43–48, 1982.

[7] S. Jalaleddine, C. Hutchens, R. Strattan, and W. Coberly, "ECG data compression techniques–a unified approach," *IEEE Trans. Biomed. Eng.*, vol. 37, pp. 329–343, Apr. 1990.

[8] G. B. Moody, K. Soroushian, and R. G. Mark, "ECG data compression for tapeless ambulatory monitors," *Comput. Cardiol.*, pp. 467–470, 1988.

[9] T. H. Linh, S. Osowski, and M. Stodolski, "On-line heart beat recognition using hermite polynomials and neuro-fuzzy network," *IEEE Transactions on Instrumentation and Measurement*, vol. 52, pp. 1224–1231, August 2003.

[10] G. D. Barlas and E. S. Skordalakis, "A novel family of compression algorithms for ECG and other semiperiodical, one dimensional, biomedical signals," *IEEE Trans. Biomed. Eng.*, vol. 43, pp. 820–828, Aug. 1996.

[11] A. Cohen, P. M. Poluta, and R. Scott-Millar, "Compression of ecg signals using vector quantization," in *Proc. of the IEEE-90 S. A. Symposium on Communications and Signal Proc.*, pp. 45–54, COMSIG–90, 1990.

[12] J. R. Cox, F. M. Nolle, H. A. Fozzard, and C. G. Oliver, "AZTEC, a preprocessing program for real time ECG rhythm analysis," *IEEE Trans. Biomed. Eng.*, vol. BME-15, pp. 128–129, Apr. 1968.

[13] B. Furht and A. Perez, "An adaptive real-time ECG compression algorithm with variable threshold," *IEEE Trans. Biomed. Eng.*, vol. 35, pp. 489–494, June 1988.

[14] C. P. Mammen and B. Ramamurthi, "Vector quantization for compression of multichannel ECG," *IEEE Trans. Biomed. Eng.*, vol. BME-37, pp. 821–825, Sept. 1990.

[15] W. C. Mueller, "Arrhythmia detection program for an ambulatory ECG monitor," *Biomed. Sci. Instrument.*, vol. 14, pp. 81–85, 1978.

[16] A. E. Pollard and R. C. Barr, "Adaptive sampling of intra-cellular and extracellular cardiac potentials with the fan method," *Med. and Biol. Eng. and Comp.*, vol. 25, pp. 261–269, 1987.

[17] M. Ishijima, S. B. Shin, G. H. Hostetter, and J. Sklansky, "Scan along polygon approximation for data compression of electrocardiograms," *IEEE Trans. Biomed. Eng.*, vol. BME-30, pp. 723–729, 1983.

[18] S. M. Jalaledding and C. G. Hutchens, "SAIES - a new ECG data compression algorithm," *J. of Clinical Eng.*, vol. 15, pp. 45–51, Jan. 1990.

[19] S. C. Tai, "SLOPE—a real-time ECG data compressor," *Medical & Biological Engineering & Computing*, vol. 29, pp. 175–179, March 1991.

[20] U. E. Ruttiman and H. V. Pipberger, "Compression of the ECG by prediction or interpolation and entropy encoding," *IEEE Trans. Biomed. Eng.*, vol. BME-26, pp. 613–623, 1979.

[21] G. Moody, "The MIT-BIH Arrhythmia Database CD-ROM (third edition)," May 1997.

[22] D. A. Huffman, "A method for the construction of minimum redundancy coders," *Proc. IRE*, vol. 40, pp. 1098–1101, 1952.

[23] Y. Zigel, A. Cohen, and A. Katz, "ECG signal compression using analysis by synthesis coding," *IEEE Trans. Biomed. Eng.*, vol. 47, pp. 1308–1316, October 2000.

[24] N. S. Jayant and P. Noll, *Digital Coding of Waveforms*. Englewood Cliffs, NJ: Prentice Hall, 1984.

[25] B. R. Shankara and I. S. N. Murthy, "ECG data compression using Fourier descriptons," *IEEE Trans. Biomed. Eng.*, vol. BME-33, pp. 428–434, 1986.

[26] W. S. Kuklinski, "Fast Walsh transform data compression algorithm for ECG application," *Med. Biol. Eng. Comput.*, vol. 21, pp. 465–473, 1983.

[27] M. E. Womble, J. S. Halliday, S. K. Mitter, M. C. Lancaster, and J. H. Triebwasser, "Data compression for storing and transmitting ECG's/VCG's," in *Proc. IEEE*, vol. 65, pp. 702–706, 1977.

[28] J. Chen, S. Itoh, and T. Hashimoto, "ECG data compression by using wavelet transform," *IEICE Trans. Inf. and Sys.*, vol. E76-D, no. 12, pp. 1454–1461, 1993.

[29] A. Ramakrishnan and S. Saha, "ECG coding by wavelet-based linear prediction," *IEEE Trans. Biomed. Eng.*, vol. 44, pp. 1253–1261, December 1997.

[30] Z. Lu, D. Y. Kim, and W. A. Pearlman, "Wavelet compression of ECG signals by the set partitioning in hierarchical trees algorithm," *IEEE Trans. Biomed. Eng.*, vol. 47, no. 7, pp. 849–856, 2000.

[31] W. S. Chen, L. Hsieh, and S. Y. Yuan, "High performance data compression method with pattern matching for biomedical ECG and arterial pulse waveforms," *Computer Methods and Programs in Biomedicine*, vol. 74, pp. 11–27, Apr. 2004.

[32] E. B. de Lima Filho, E. A. B. da Silva, M. B. de Carvalho, W. S. da Silva Junior, and J. Koiller, "Electrocardiographic signal compression using multiscale recurrent patterns," vol. 52, no. 12, 2005.

[33] P. S. Hamilton, "Adaptive compression of the ambulatory electrocardiogram," *Biomedical Inst. and Tech.*, pp. 56–63, Jan. 1993.

[34] A. Iwata, Y. Nagasaka, and N. Suzumura, "Data compression of ECG using neural network for digital holter monitor," *IEEE Eng. in Med. and Biolo. Mag.*, pp. 53–57, Sept. 1990.

[35] P. S. Hamilton and W. J. Tompkins, "Quantitative investigation of QRS detection rules using the MIT/BIH arrhythmia database," *IEEE Trans. Biomed. Eng.*, vol. BME-33, pp. 1157–1165, 1986.

[36] P. P. Vaidyanathan, *Multirate Systems and Filter Banks*. Englewood Cliffs, NJ: Prentice Hall, 1993.

[37] H. Abbas, "Time series analysis for ECG data compression," in *ICASSP '99. Proceedings.*, vol. 3, pp. 1537–1540, March 1999.

[38] R. Istepanian, L. Hadjileontiadis, and S. Panas, "ECG data compression using wavelets and higher order statistics methods," *IEEE Transactions on Information Technology in Biomedicine*, vol. 5, pp. 108–115, June 2001.

[39] M. Vetterli, P. Marziliano, and T. Blu, "Sampling signals with finite rate of innovation," *IEEE Transactions on Signal Processing*, vol. 50, pp. 1417–1428, June 2002.

[40] M. Vetterli, P. Marziliano, and T. Blu, "Sampling discrtete-time piecewise bandlimited signals," in *Sampling Theory and Applications Workshop*, (Orlando, USA), pp. 97–102, May 2001.

[41] P. Marziliano, *Sampling Innovations*. PhD thesis, Swiss Federal Institute of Technology - Lausanne, Switzerland, April 2001.

[42] P. Marziliano, M. Vetterli, and T. Blu, "Sampling and exact reconstruction of bandlimited signals with additive shot noise," *IEEE Transactions on Information Theory*, vol. 52, pp. 2230–2233, May 2006.

[43] I. Maravic, *Sampling methods for parametric non-bandlimited signals: extensions and applications*. PhD thesis, Swiss Federal Institute of Technology - Lausanne, Switzerland, September 2004.

[44] G. H. Golub and C. F. V. Loan, *Matrix Computations*. London: John Hopkins University Press, 1996.

Appendix A

The MIT-BIH Arrhythmia Database

The database used in this work is a collection of files from the MIT-BIH Arrhythmia Database CD-ROM (third edition) [Moody, 1997].

The source of the ECGs included in the MIT-BIH Arrhythmia Database is a set of over 4000 long-term Holter recordings that were obtained by the Beth Israel Hospital Arrhythmia Laboratory between 1975 and 1979. Approximately 60% of these recordings were obtained from inpatients. The database contains 23 records (numbered from 100 to 124 inclusive with some numbers missing) chosen at random from this set, and 25 records (numbered from 200 to 234 inclusive, again with some numbers missing) selected from the same set to include a variety of rare but clinically important phenomena that would not be well-represented by a small random sample of Holter recordings.

The first group is intended to serve as a representative sample of the variety of waveforms and artifact that an arrhythmia detector might encounter in routine

clinical use. A table of random numbers was used to select tapes, and then to select half-hour segments of them. Segments selected in this way were excluded only if neither of the two ECG signals was of adequate quality for analysis by human experts.

Records in the second group were chosen to include complex ventricular, junctional, and supraventricular arrhythmias and conduction abnormalities. Several of these records were selected because features of the rhythm, QRS morphology variation, or signal quality may be expected to present significant difficulty to arrhythmia detectors; these records have gained considerable notoriety among database users. The subjects were 25 men aged 32 to 89 years, and 22 women aged 23 to 89 years. Records 201 and 202 came from the same male subject.

Each record in this directory is slightly over 30 minutes in length. Each signal file contains two channels of ECG signals sampled at 360 Hz. Each sample is represented by 12-bit two's complement amplitude. To each signal file a header file and a reference annotation file are attached. The header files include information about the leads used, the patient's age, sex, and medications. The reference annotation files include beat, rhythm, and signal quality annotations.